PVTx Measurements and Crossover Equation of State of Pure *n*-Hexane and Dilute Aqueous *n*-Hexane Solutions in the Critical and Supercritical Regions

I. M. Abdulagatov,[†,‡] A. R. Bazaev,[†] J. W. Magee,[‡] S. B. Kiselev,[*,§] and J. F. Ely[§]

Institute for Geothermal Problems of the Dagestan Scientific Center of the Russian Academy of Sciences, 367003 Makhachkala, Shamilya Str. 39-A, Dagestan, Russia, Physical and Chemical Properties Division, National Institute of Standards and Technology, 325 Broadway, Boulder, Colorado 80303, and Chemical Engineering Department, Colorado School of Mines, Golden, Colorado 80401-1887

The *PVTx* relationship of aqueous *n*-hexane solutions (0.0201, 0.082, and 0.8500 mole fraction of *n*-hexane) has been measured in the near-critical and supercritical regions with a constant-volume piezometer. Measurements were made on the critical isotherm of pure water 647.1 K with pressures ranging from 8 to 33 MPa. The total uncertainties of density, pressure, temperature, and composition measurements are estimated to be less than 0.16%, 0.05%, 15 mK, and 0.001 mole fraction, respectively. The Krichevskii parameter was estimated (124.4 ± 20 MPa) from direct measurements of the $P-x$ dependence along the critical isotherm-isochore of pure water. The measured *PVTx* data were used to calculate partial molar volumes at infinite dilution for *n*-hexane $\bar{V}_2^\infty$ in near-critical water. The asymptotic behavior of the partial molar volume along the solvent's (pure water) critical isotherm-isobar was studied. The molar volume values for the dilute H_2O + *n*-C_6H_{14} mixture along the critical isotherm-isochore of pure water were also used to estimate the critical exponent of partial molar volume $\bar{V}_2^\infty \propto x^{-\epsilon}$ ($\epsilon = 0.795 \pm 0.001$). Using our new *PVTx* data together with data obtained in other studies, we developed a crossover Helmholtz free-energy model (CREOS) for dilute aqueous *n*-hexane solutions in wide temperature and pressure ranges around the vapor−liquid critical points. The CREOS model requires only the critical locus as an input and represents all available experimental *PVTx* data for a dilute H_2O + *n*-C_6H_{14} mixture with an average absolute deviation (AAD) of about 0.50−0.65% in the temperature and density ranges $0.98T_c(x) \le T \le 1.15T_c(x)$ and $0.35\rho_c(x) \le \rho \le 1.65\rho_c(x)$, respectively, and concentrations up to 0.05 mole fractions of *n*-hexane. The accuracy and predictive capability of the crossover model was confirmed by comprehensive comparison of present crossover EOS for the pure *n*-hexane with the available experimental data in the critical and supercritical regions.

1. Introduction

Thermodynamic properties of hydrocarbons in water at high temperatures and high pressures are of considerable interest in a number of industrial applications. Since water's dielectric constant varies from a room-temperature value of 80 to a value of 5 at its critical point, it can solubilize most nonpolar organic compounds including most hydrocarbons and aromatics at temperatures starting at 473 and extending to the critical point.[1,2] Therefore, supercritical water (SCW) has been proposed as a solvent and as a reaction medium for a number of technological applications such as coal conversion,[3] organic synthesis,[4] environmentally friendly destruction of toxic and hazardous wastes,[5−9] including chemical weapons and the cleanup of nuclear processing sites,[10−12] SCW oxidation processes,[13,14] and extraction of organics from environmental solids.[15−19] Water + hydrocarbon systems may also serve as model systems that are useful for the development of processes such as the hydrolysis of plastic, synthetic fibers, or polycarbonates for recycling.[20]

Exploration of the possibilities offered by SCW solubility requires an accurate and detailed knowledge of the fluid thermodynamic properties, particularly *PVTx* relation and equation of state of the near-critical mixtures. The present technological advancement in the use of high temperature and high pressure in chemical industries would be well-served by an understanding of the phase and *PVTx* relations in water + hydrocarbon mixtures. *PVTx* data for water + hydrocarbon systems provide additional information on the effects of temperature, pressure, and composition on the thermodynamic behavior in such systems, which could lead to improved understanding of processes near the solvent critical point. However, *PVTx* data for the water + hydrocarbon systems under supercritical conditions are scarce and there is no reliable nonclassical equation of state that adequately describes the anomalous thermodynamic behavior of the near-critical and supercritical aqueous hydrocarbon mixtures.

The thermodynamic behavior of dilute mixtures in the vicinity of a solvent's (water) critical point is also of considerable theoretical importance. Much of the theoretical work on supercritical solubility has focused upon

* To whom correspondence should be addressed. Phone: (303) 273-3190. Fax: (303) 273-3730. E-mail: skiselev@mines.edu.

[†] Institute for Geothermal Problems of the Dagestan Scientific Center of the Russian Academy of Sciences.

[‡] National Institute of Standards and Technology.

[§] Colorado School of Mines.

10.1021/ie049339a CCC: $30.25
Published on Web 02/02/2005

Table 1. Summary of the Thermodynamic Properties Measurements for Aqueous *n*-Hexane Mixtures

first author	year	property	method	temperature range (K)	pressure range (MPa)	concentration range (mol. fr.)
Abdulagatov[34]	1994	$PVTx$, B_m, C_m	CVP[b]	523−623	2−16	0.198−0.9398
Abdulagatov[35]	2001	$PVTx$, B_{12}	CVP[b]	643−651	8−35	0.0021−0.0138
Degrange[36]	1998	$PVTx$, H^E	VTD[a]	298−675	up to 33	infinite dilution
Yiling[37]	1991	$PVTx$	CVA,[c] VVA[d]	550−700	20−200	0.4−0.8
De Loos[43,44]	1982	PTx		600−675	25−170	n.a.
Majer[57]	1999	$\bar{V}_2^\infty$	$Lim_{x\to 0}{}^{\phi} V_m$	573−623	up to 30	infinite dilution
Wormald[54−56,109]	1980	B_{12}	FMC[e]	363−698	up to 12	0.369−0.611
	1983	Φ_{12}				
	1988	H^E				
	1996					
Smith[110]	1984	H^E	FMC[e]	363−423	0.101325	0.42−0.47
Kamilov[38]	1996	$PVTx$, C_VVTx T_S, ρ_S	HTHPAC[f]	398−622	up to 25	0.385−0.879
Kamilov[39]	2001	C_VVTx	HTHPAC[f]	463−522	up to 6	0.62−0.994
Kamilov[40]	1997	$PVTx$, C_VVTx, T_S, ρ_S	HTHPAC[f]	373−780	up to 60	0.25−0.933
Stepanov[41]	1997	C_VVTx, T_S, ρ_S	HTHPAC[f]	380−495.8	up to 25	0.256, 0.615
Tsonopoulos[45]	1983	three-phase $P-T$		313−422	0.0454−3.52	0.00123−0.11
this work	2004	$PVTx$	CVP	647.1	9−34	0.02−0.85

[a] VTD, vibrating-tube densimeters. [b] CVP, constant-volume piezometer. [c] CVA, constant-volume autoclave. [d] VVA, variable-volume autoclave. [e] FMC, flow mixing calorimeter. [f] HTHPAC, high-temperature and high-pressure adiabatic calorimeter. [g] FM, flow method.

relating the infinite dilution properties, for example, negatively and positively diverging solute partial molar volume in mixtures in the immediate vicinity of the solvent's critical point, path-dependence solvent properties in near-critical systems, and microstructure of infinite dilute supercritical aqueous solutions.[21−33]

The main objectives of this paper are to provide new reliable experimental volumetric, $PVTx$ data and to develop a new theoretically based crossover equation of state for pure *n*-hexane and dilute aqueous *n*-hexane mixture in the sub-, near-, and supercritical regions. We proceed as follows. In section 2 we review the existent experimental data for H_2O + n-C_6H_{14} mixtures. In section 3 we describe an experimental procedure used in this work. A brief review of the previous equations of state mixtures is given in section 4, and in section 5 we describe a crossover free-energy model for H_2O + n-C_6H_{14}. The results and discussion are presented in section 6, and the conclusions are given in section 7.

2. Literature Review of the Experimental Thermodynamic Properties of H_2O + n-C_6H_{14} Mixture

The thermodynamic properties of H_2O + n-C_6H_{14} solutions have been reported by many authors. Table 1 shows the available thermodynamic data sets for H_2O + n-C_6H_{14} mixtures. In this table the first author and the year published are given together with the method employed, and the temperature, pressure, and concentration ranges. The available experimental critical curve data sets are given in Table 2. A brief analysis of the different data sets is given below.

2.1. *PVTx* Measurements. Abdulagatov et al.[34] reported $PVTx$ data for H_2O + n-C_6H_{14} mixtures along the three isotherms (523.15, 573.15, and 623.15) K for 12 compositions between 0.1968 and 0.9398 mole fraction of n-C_6H_{14}. Pressures ranged between 2 and 16 MPa and densities from 9 to 496 kg·m^{-3}. Newer more precise experimental $PVTx$ data for infinitely dilute H_2O + n-C_6H_{14} mixtures near the solvent (pure water) critical point were reported recently by Abdulagatov et al.[35] These experimental $PVTx$ data provide a stringent test of scaling models. Measurements were made at five near-critical and supercritical isotherms of pure water 643.05, 645.05, 647.05, 649.05, and 651.05 K and at pressures from 8 to 35 MPa for four compositions, namely: 0.0021, 0.0050, 0.00850, and 0.0138 mole fraction of *n*-hexane. The uncertainty in density measurements reported by Abdulagatov et al.[34,35] is 0.16%. Degrange[36] also measured $PVTx$ properties for infinite dilution mixtures of water + hydrocarbon (benzene, toluene, *n*-hexane, and cyclohexane) in the temperature range from 298.15 to 675 K and pressures up to 33 MPa. The measurements of density differences between hydrocarbon and water were carried out as a function of concentration using vibrating-tube densimeters.

Table 2. Summary of the Critical Properties (T_C, P_C, ρ_C) Measurements for Aqueous *n*-Hexane Mixtures

first author	year	temperature range (K)	density range (kg·m^{-3})	pressure range (MPa)
Connolly[1]	1993	625 ± 2		31.4 ± 1
Yiling[37]	1991	663.2; 673.3		93.0; 111.0
De Loos[43,44]	1982	610−675		15−140
Kamilov[39]	2001	UCEP	UCEP	UCEP
Tsonopoulos[45]	1983	UCEP		UCEP
Brunner[46]	1990	414−647.1		up to 40
Brunner[46]	1990	UCEP		UCEP
Roof[47]	1970	UCEP		UCEP
Rebert[48]	1967	UCEP		UCEP
Scheffer[49]	1914	UCEP		UCEP

Yiling et al.[37] reported mixture $PVTx$ data for H_2O + n-C_6H_{14} in the temperature range from 550 to 700 K at pressures from 20 to 200 MPa. Measurements were made with a constant volume piezometer and a variable volume autoclave. The uncertainties of the measured values of volume, pressure, and concentration were 1%, 0.2 MPa, and 0.5%, respectively. Kamilov et al.[38−40] used a high-temperature−high-pressure adiabatic calorimeter to measure $PVTx$ properties of H_2O + n-C_6H_{14} mixtures. The authors claimed uncertainties of the pressure, density, and concentration measurements were 0.09%, 0.10%, and 0.0005 mole fractions, respectively.

2.2. Phase Equilibrium Measurements. Figure 1 shows the $P-T$ phase diagram for the water + *n*-hexane mixture. This figure includes all of the available experimental three-phase data, low and upper critical curves, UCEP, and vapor-pressure curves for the pure components. The phase behavior of the H_2O + n-C_6H_{14}

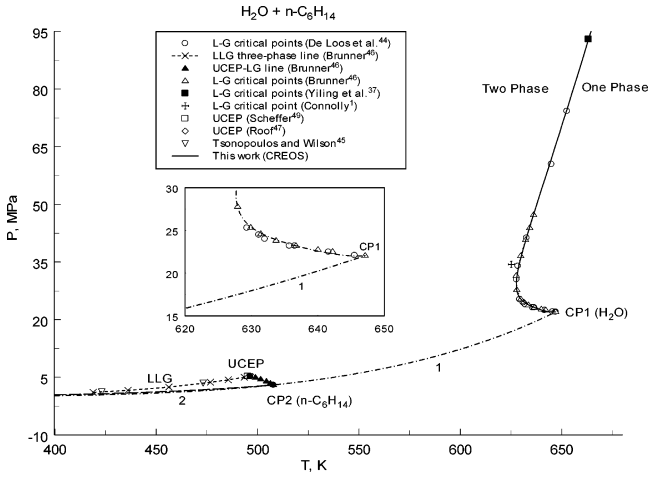

Figure 1. Pressure−temperature phase diagram for the H_2O + n-C_6H_{14} mixture. CP1, critical point of pure water; CP2, critical point of pure n-hexane; 1, vapor-pressure curve calculated with the IAPWS[67] formulation for pure water; 2, vapor-pressure curve calculated with the multiparametric EOS of Span.[93]

mixture belongs to type III mixtures in accordance with the classification scheme of van Konynenburg and Scott.[41]

Phase transition phenomena (L−L−V, L−L, and L−V) in water + n-hexane mixtures were studied by Kamilov et al.[38−40] and Stepanov et al.[42] using calorimetric (C_V) experiments. They measured saturated temperatures T_S and densities ρ_S at phase transition points using quasi-static thermogram technique. The measured densities on the three-phase curve define a smooth curve, with a temperature maximum at 495.82 K. This maximum temperature corresponds to the UCEP (upper critical end point), where the densities of liquid and vapor mixtures in the three-phase equilibrium become identical or as the intersection of the critical curve (L = G) and the three-phase solubility curve (L−L−G). comparison of experimental values of densities on the two-phase boundary (x = 0.61 mole fraction of n-hexane) derived from calorimetric ($PVTx$) measurements by Kamilov et al.[39]and from thermal ($PVTx$) measurements by Yiling et al.[37] show that the differences of about 0.6%.

A number of phase equilibrium (PTx measurements along the phase equilibrium curve) studies have been made by Yiling et al.,[37] de Loos et al.,[43,44] Tsonopoulos and Wilson,[45] Brunner,[46] Roof,[47] Rebert and Hayworth,[48] and Scheffer.[49] All of the measurements were performed at temperatures up to the critical point of pure water. de Loos et al.[44] have made measurements of PTx properties on the phase boundary for the seven compositions in the temperature range from 600 to 675 K and at pressures from 15 to 170 MPa.

The two-phase equilibrium surface in PTx space has been measured by Yiling et al.[37] in the temperature range from 550 to 700 K and with pressures between 20 and 240 MPa. Two types of autoclaves with constant and variable volumes of about 60 cm^3 and equipped with sapphire windows were used. Measurements were made for compositions between 0.4 and 0.8 mole fraction of water. From the boundary curves, the binary critical curves have been derived. Points on the phase boundary were derived from "breakpoints" on $P-T$ isochores. To determine the phase equilibria, the "synthetic" method was applied: known amounts of the two components were heated in an autoclave of constant volume and the pressure increase with temperature was recorded. A discontinuity (a "breakpoint") indicated the transition to homogeneous one-phase behavior and to an almost linear $P-T$ isochore. Each breakpoint was one point on the three-dimensional binodal surface. It could also be determined by visual observation through the sapphire windows. A set of such breakpoints was obtained at different volumes but constant compositions. The autoclaves were made from a high-strength nickel-base alloy with 30 cm length and 60 mm o.d. and 20 mm i.d.. They were mounted horizontally and had a series of heating and cooling jackets to control temperature gradients. The sample temperature was determined by thermocouples within the sample and within the autoclave wall. Magnetic stirring was provided for the sample space. The uncertainties of the temperature, pressure, mole fraction, and volumes were 0.5 K, 0.2 MPa, 0.5%, and 1%, respectively.

The PTx values on the liquid−liquid−gas three-phase lines and on both branches of the critical curve $P_C(T)$ for water + n-alkane mixtures have been measured by Brunner[46] from 414 K to the critical temperature of pure water at pressures up to 40 MPa. Phase equilibria were measured by de Loos et al.[43] at high values of composition of n-hexane and to moderate pressures by Rebert and Hayworth.[48]

2.3. Isochoric Heat Capacity Measurements. Experimental $C_{V,x}$ data have been reported by Kamilov et al.[38−40] and Stepanov et al.[42] near the liquid−gas, liquid−liquid, and liquid−liquid−gas phase transition points. Kamilov et al.[38] reported the isochoric heat capacity data along the critical isochores and coexistence curves. Extensive $C_{V,x}$ measurements for six compositions (0.6146, 0.7965, 0.9349, 0.9775, 0.9892, and 0.9940 mole fraction of n-hexane) near the (L−L−V) and (L−L) and (L−V) phase transition curves have been reported by Kamilov et al.[39] These measurements cover the range of temperature from 463 to 522 K at pressures up to 6 MPa and densities between 259 and 312 kg·m^{-3}. The values of temperature, pressure, and density at the upper critical end point (UCEP) were determined from the measurements. Two peaks or jumps in the isochoric heat capacity were found. The discontinuity in $C_{V,x}$ behavior at the intersection of the phase boundary curve is connected with (L−L) and (L−V) phase transitions occurring in a binary water + n-C_6H_{14} mixture heated in a closed volume. Heating the three phase (L−L−G) water + n-C_6H_{14} mixture can lead to three different sequences of phase transitions, depending on the fill coefficient (ratio of the volume of the mixture to the volume of the calorimeter at ambient temperature) or the average fill density (ratio of the mass of mixture to the volume of the calorimeter at ambient temperature), and the n-C_6H_{14} concentration in the initial mixture (see Kamilov et al.[39]). For the first time Kamilov et al.[39] experimentally studied the temperature dependence behavior of $C_{V,x}$ near the UCEP. The uncertainty in the isochoric heat capacity measurements was 1.0−1.5%.

2.4. Critical Properties of Aqueous *n*-Hexane Mixtures. Aqueous systems show unusually shaped critical lines. The mutual solubility of hydrocarbons and water is very low and the three-phase equilibrium line occurs at significantly higher pressures than the vapor-pressure curve of the pure alkanes (see Figure 1). The liquid−gas critical curve that connects the critical end point of the three-phase line and the critical point of one of the components (n-hexane) is rather short. There

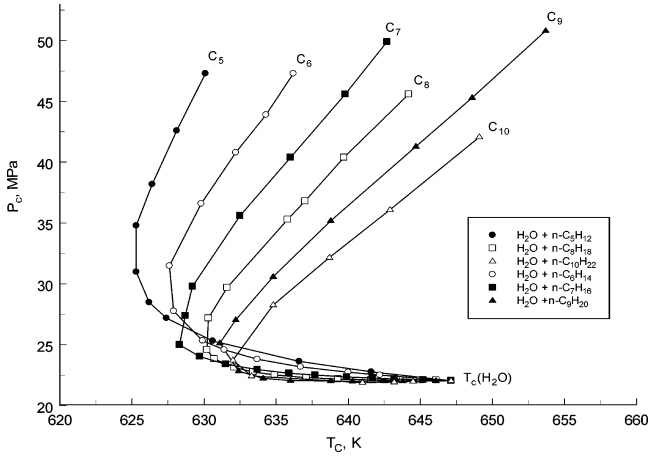

Figure 2. $P_C - T_C$ projection (upper branch) of the critical curves for H_2O + *n*-alkane mixtures (Brunner[46]).

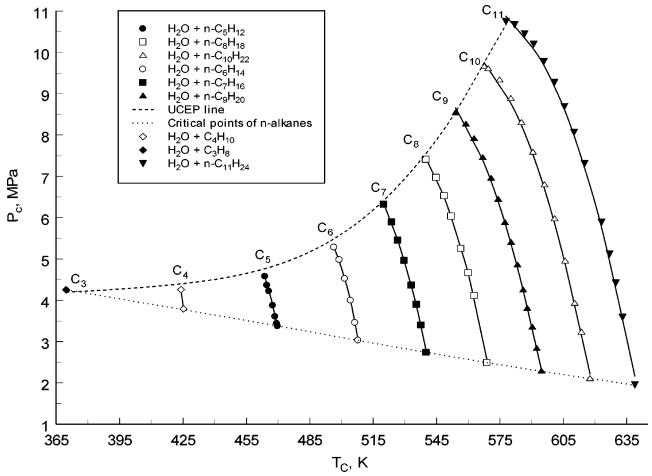

Figure 3. $P_C - T_C$ projection (lower branch) of the critical curves for H_2O + *n*-alkane mixtures (Brunner[46]).

is no continuous critical curve between the pure H_2O and pure *n*-hexane critical points (see Figure 1). One critical curve (lower critical curve) goes from the point T_C of *n*-hexane and terminates at the upper critical point (UCEP) three-phase L−L−V equilibrium end points. The other critical curve (upper critical curve), originating from the pure water critical point T_C extends toward very high pressures and has a minimum with respect to temperature at the point where the two-phase region separates into two parts (see Figure 1). The shape of the critical curves for water + *n*-alkanes changes systematically from system to system (see Figures 2 and 3, Brunner,[46] and de Loos et al.[43,44]). It shifts to lower pressures with the *n*-alkane carbon number. The temperature at the critical locus minimum does not differ very much. The temperature at the critical end point is noticeably less than pure alkane's critical temperatures for the mixtures with butane and heavier alkanes. The critical curves for water + *n*-alkane mixtures are interrupted and show gas−gas equilibria of the second kind (de Loos et al.[43,44] and Brunner[46]). de Loos et al.[43] have measured the phase equilibria (*PTx*) and the critical properties (P_C, T_C, x_C) in H_2O + *n*-C_6H_{14} mixtures in the temperature range from 610 to 675 K and at pressures from 15 to 140 MPa.

From the boundary curves, the binary critical curves have been derived by Yiling et al.[37] The critical curve passes through temperature minima at $T_m = 628$ K and $P_m = 31$ MPa. The derived values of the critical parameters for water + *n*-hexane are given in Figures 4a−c and 5 in the $T_C - x$, $\rho_C - x$, $\rho_C - x$, and $P_C - T_C$ projections, respectively, together with values measured by other authors.

The critical curve of the water + *n*-hexane mixtures has been derived from phase equilibrium measurements by de Loos et al.[43,44] using a visual method (by observing the behavior of the meniscus). They found that the critical curve of the mixture starts at the critical point of pure water ($T_C = 647.1$ K and $P_C = 22.1$ MPa) and runs via a temperature minimum at $T_m = 627.8 \pm 0.2$ K and $P_m = 31 \pm 2$ MPa to higher pressures. They showed also that the critical line changes systematically with the carbon number of the *n*-alkane[43,44,46] (see Figures 2 and 3). The temperature of the disappearance of the second fluid phase was measured to accuracy within ±0.1 K. The pressure was measured with accuracy within ±0.02 MPa at pressures up to 40 MPa and ±0.05 MPa at higher pressures. The uncertainty in the concentration measurements is estimated to be 0.002 mole fraction. The measured values of the critical parameters (T_C and P_C) as a function of composition x are shown in Figures 4a,b. The critical curves for these mixtures in $P_C - T_C$ projection are given in Figure 5 together with the vapor-pressure curve for pure water near the critical point. With increasing number of carbon atoms in the *n*-alkane, the critical line is shifted to lower pressures and higher values of x (see Figure 2). The temperature of the temperature minimum of the critical curves is almost the same in all H_2O + *n*-alkane mixtures.[44,46,50]

The $P_C - T_C$ projections of the critical curves for 23 binary mixtures of water + *n*-alkanes with *n*-alkane-carbon numbers $i = 1$ to 12 and $i = 14$, 16, 18, 20, 24, 25, 26, 28, 30, 32, and 36 were measured by Brunner.[46] Measurements were performed in a 30 cm^3 cylindrical high-pressure optical cell. The operating pressure of the cell is 200 MPa at 750 K. The uncertainties of pressure and temperature measurements at phase boundary appearance or disappearance are 0.1% and 0.2 K, respectively. The total uncertainty of the critical pressure measurements to be estimated 0.4%. The critical parameters for water + hydrocarbon mixtures have been also measured by Rebert and Hayworth[48] (*n*-C_6H_{14}, cyclohexane, and benzene) and Roof[47] (propane, butane, *n*-pentane, *n*-C_6H_{14}, *n*-octane, *n*-nonane, *n*-decane, benzene, and toluene). These data are also presented in Figure 5.

The available literature data on the UCEP parameters for water + *n*-hexane mixtures are given in Table 3. The results by Kamilov et al.[39] for the UCEP temperature $T_{UCEP} = 495.82$ K and UCEP pressure $P_{UCEP} = 5.250$ MPa are in good agreement (differences are $\Delta T_{UCEP} = 0.63$ K and $\Delta P_{UCEP} = 0.02$ MPa) with the values reported by other authors.[45−49] However, the maximum deviation between the UCEP temperature and the data reported by Tsonopoulos and Wilson[45] was 0.88 K and the UCEP pressure differs by 0.045 MPa (Roof[47]). For the first time Kamilov et al.[39] reported a value of the UCEP density $\rho_{UCEP} = 259.94$ kg·m^{-3}. The UCEP is located about 8 K below the critical temperature ($T_C = 507.85$ K) and about 2.22 MPa above the critical pressure ($P_C = 3.03$ MPa) of *n*-hexane.

2.5. Other Thermodynamic Property Measurements. Degrange[36] measured enthalpies for infinitely dilute water + hydrocarbon mixtures (benzene, toluene, *n*-hexane, and cyclohexane) in the temperature range

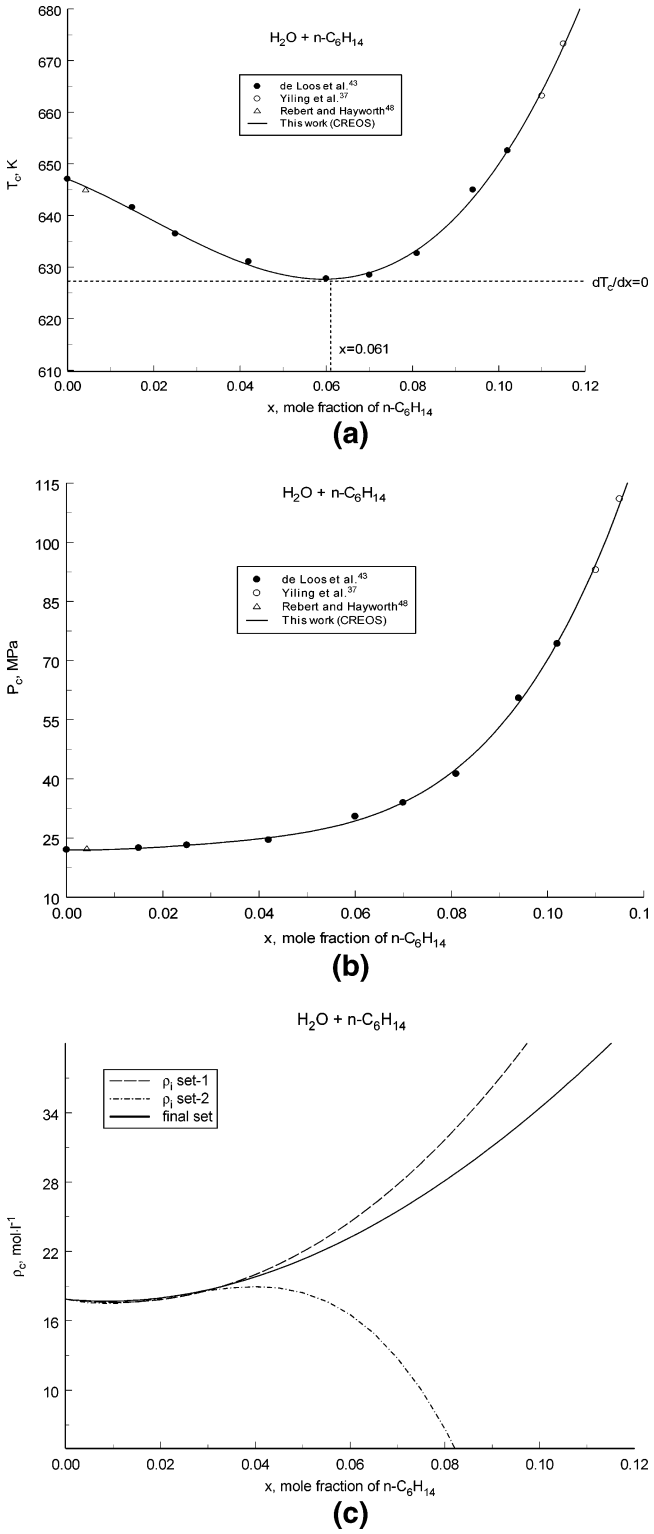

Figure 4. (a–c) Measured and calculated critical temperatures (a), critical pressures (b), and critical densities (c) for H_2O + n-C_6H_{14} mixtures as a function of concentration.

298.15–675 K with pressures up to 33 MPa. The measurements of enthalpies were carried out as a function of concentration using vibrating-tube densimeters.

The excess vapor enthalpy H^E of water + n-alkane vapor has also been measured by Wormald et al.[54–56] using a flow mixing calorimeter. Temperatures ranged from 363 to 698 K at a pressure of 16 MPa for compositions from 0.369 to 0.611 mole fraction of

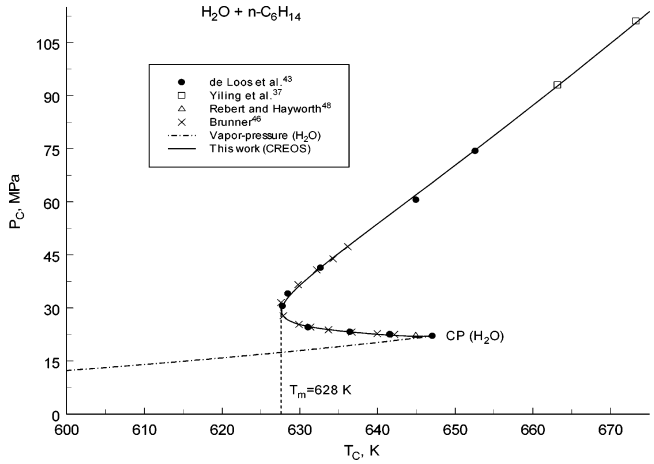

Figure 5. Experimental and calculated critical locus ($P_C - T_C$) for H_2O + n-C_6H_{14} mixtures together with vapor-pressure curve for pure water (IAPWS[67]).

Table 3. Values of the UCEP Temperature, Pressure, and Density for the H_2O + n-C_6H_{14} Mixtures

T_{UCEP} (K)	P_{UCEP} (MPa)	ρ_{UCEP} (kg·m^{-3})	references
495.82	5.250	259.94	Kamilov et al.[39]
496.70	5.270		Tsonopoulos and Wilson[45]
496.40	5.282		Brunner[46]
496.48	5.295		Roof[47]
495.15	5.275		Rebert and Hayworth[48]
495.21	5.274		Scheffer[49]

n-alkane. Cross-second virial coefficients B_{12} and cross-isothermal Joule-Thomson coefficients Φ_{12} for the water + n-hexane were derived from the excess enthalpy data. An alternative to calorimetric measurements (H^E) are accurate $PVTx$ measurements, which can be used for testing of the two types of measurements. Wormald et al.[54] also constructed a high-pressure flow calorimeter for the measurements of the H^E at temperatures up to 700 K and used it to measure H^E for H_2O + n-pentane, + n-C_6H_{14}, + n-heptane, and + n-octane. The high-temperature measurements were used to calculate the excess molar volumes V^E and compressibility factors for the water + n-C_6H_{14} mixtures.

Most recently a data set of partial molar volumes at infinite dilution was obtained for the water + n-C_6H_{14} mixtures by Majer et al.[57] at temperatures from 573 to 623 K and at pressures to 30 MPa from densimetric measurements.

3. Experimental Procedure

The methods and procedures used in this study are the same as those employed previously in the study of pure water, n-alkanes, and water + n-alkane mixtures.[34,35,58–66] A detailed description of the apparatus and the experimental procedures used for the $PVTx$ measurements has been given previously in our series publications,[34,35,58–66] and only essential information will be given here. The measurements were made using a constant-volume high-pressure piezometer. The high-pressure piezometer is constructed of heat- and corrosion-resistant high-strength alloy EI-43BU-VD (nickel, 77.00%; chromium, 19.84%; titanium, 2.82%; aluminum, 0.8%; iron, 0.59%; silicon, 0.44%; copper, 0.01%). The inner volume of the piezometer was calculated by taking into consideration corrections for elastic pressure deformation and thermal expansion and was calibrated

by filling it with distilled water and then withdrawing the water and weighing. The mass of the water withdrawn $m(H_2O)$ yielded the volume of the piezometer $V_{T_0P_0} = m(H_2O)/\rho(H_2O)$ from the well-established density $\rho(H_2O)$ of water at temperature T_0 and pressure P_0 of the calibration. The density of water was calculated with a standard reference equation of state (IAPWS, Wagner and Pruss[67]) at a temperature of $T_0 = 673.15$ K and a pressure of $P_0 = 38.40$ MPa. The uncertainty of the density calculation from IAPWS[67] formulation at this condition is $\delta\rho_{H_2O} = 0.1\%$. All masses were determined with an uncertainty of 5×10^{-4} g or 0.003−0.04%. Therefore, in the worst case the volume of the piezometer at this temperature T_0 and pressure P_0 was determined with uncertainty of 0.14% ($\delta V_{P_0V_0} = \delta m + \delta\rho_{H_2O}$). The volume at these conditions $V_{P_0T_0} = (32.802 \pm 0.045)$ cm^3. This calibration was checked using other pure fluids. The resulting value of the piezometer volume was essentially the same as determined before with water (difference is 0.12%).

It is necessary to know the volume of the piezometer, V_{PT}, at a given temperature T and pressure P, for the purpose of calculating densities $\rho(T,P) = m/V_{PT}$. The effect of the temperature and pressure on the piezometer volume V_{PT} was estimated using the thermal expansion coefficient α of alloy EI-43BU-VD and the pressure expansion coefficient β of the piezometer. Variations of the piezometer volume V_{PT} with temperature T and pressure P were calculated with the equation (Tsiklis et al.[68])

$$V_{PT} = V_{P_0T_0}[1 + 3\alpha(T - T_0) + \beta(P - P_0)] \qquad (1)$$

where $\alpha = 1.56 \times 10^{-5}$ K^{-1} is the thermal expansion coefficient of the piezometer material, which is almost independent of temperature in the range from 370 to 700 K, and $\beta = 3.51 \times 10^{-5}$ MPa^{-1} is the pressure expansion coefficient of the piezometer. The values of α and β were determined also by using a calibration procedure with pure water between 373 and 675 K at pressures up to 100 MPa. The maximum uncertainty in volume of the piezometer at a given temperature and pressure V_{PT} is related to the measured uncertainties of $V_{P_0T_0}$ (0.14%), uncertainty of α and β, which was 10%, and uncertainties in pressure (0.05%) and temperature (0.0015%) as

$$\delta V_{PT} = \delta V_{P_0V_0} + \frac{V_{P_0T_0}}{V_{PT}}[3\alpha[(T - T_0)\delta\alpha + T\delta T] + \beta[(P - P_0)\delta\beta + P\delta P]] \qquad (2)$$

In the worst case (at maximum pressure 100 MPa and maximum temperature 673.15 K) the uncertainty in V_{TP} determination from eq 2 is 0.16%. Even if the values of α and β were determined with uncertainty of 20%, the uncertainty in V_{TP} is not worse than 0.18%. The pressure dependence of the piezometer volume ΔV_P was also calculated from the Lave formula (Keyes and Smith[69]) for the cylinder. The differences between experimentally determined values of ΔV_P and those calculated with Lave formula are within 0.1%.

Stirring of sample in the piezometer was accomplished with the aid of a steel ball that was moved by the oscillation of the thermostat. The fluid temperature was measured with a 10 Ω platinum resistance thermometer (PRT-10). The maximum uncertainty in the measured temperature was 15 mK. The temperature inside the thermostat was maintained uniform to within 5 mK with the aid of guard heaters located between the thermostat walls and regulating heaters, which were mounted inside the thermostat. The temperature inside the thermostat and the fluid temperature were controlled automatically (Bazaev[70]). The thermostat has double walls with an inside volume of 65 dm^3. The heating elements were arranged between the walls. To minimize temperature gradients in the air thermostat, two electrically driven high-speed fans were used. The pressure in the piezometer was measured with an oil dead-weight gauge with an estimated uncertainty of 0.05%.

The present experimental apparatus had no noxious ("dead") volumes.[34,35,58−66] Taking into account the uncertainties of measurements of temperature, pressure, and concentration, the total experimental uncertainty of density was estimated to be 0.163−0.20% ($\delta\rho = \delta V_{PT} + \delta m$) depending on the temperature and pressure. To check the reproducibility of the experimental values, some of the measurements were repeated at selected temperature and pressure several times. The reproducibility of the (P,T)-data is better than ±0.1%. To check and confirm the accuracy of the measurements, *PVT* measurements were made on pure water. The measured values of density and pressure for the two selected supercritical isotherms, 653.15 and 673.15 K, of pure water were compared with the data calculated from the IAPWS[67] formulation for pure water. The absolute average deviation (AAD) between measured values of density and calculations with IAPWS[67] is AAD = 0.14%.

Pressure was measured as a function of density at fixed temperature. The piezometer was filled at room temperature, sealed off, and heated along the quasi-isochore. After the cell reached the desired temperature, the sample was maintained in the piezometer for 2−3 h. After it reached equilibrium (pressure in the piezometer at given temperature and density stabilized) at the desired temperature, the sample pressure was recorded.

4. Analytical Equations of State for Water + *n*-Hexane Mixtures

Different types of EOS have been used in the literature to represent thermodynamic properties of water + n-hexane solutions, but all of them are classical, analytical type EOS and fail to reproduce the singular behavior of the thermodynamic properties of pure fluids and fluid mixtures in the critical region. Table 4 summarizes available EOS for water + n-hexane published in the literature and their features. Briefly, a modified Soave−Redlich−Kwong (MSRK) equation of state with an exponent-type mixing rule[71] for the energy parameter and a conventional mixing rule for the size parameter was applied to correlate the phase equilibria for four binary mixtures of water + hydrocarbon (benzene, n-hexane, n-decane, and dodecane) systems at high temperatures and pressures by Haruki et al.[72,73] The perturbation type of the equation of state with repulsion and an attraction term with square-well potential for intermolecular interaction was used by Neichel and Franck[51] for water + n-alkane (C_1 to C_6, and C_{12}) mixtures. The three adjustable parameters w_{ij}, k_ϵ, and k_σ for the square-well molecular interaction potential were fitted to the critical curves data.

Table 4. Previous EOS for H_2O + n-C_6H_{14} Mixtures

first author	year	temperature range (K)	pressure range (MPa)	structure of the EOS	number of adjustable parameters	data used in the development
Haruki[72,73]	1999 2000	603−633	up to 150	MSRK[a]	3	VLE
Neichel[51]	1996	670	up to 200	PTSWP[b]	3	critical curves data
Heilig[52,53]	1990					
Tsonopoulos[45]	1983	470	3.5	RKJZ[c]	1	solubility data
Eubank[111]	1994	n.a.	n.a.	PR[d]	1	solubility data
Victorov[50]	1991	n.a.	n.a.	QCGCH[e]	5	VLE

[a] MSRK, modified Soave−Redlich−Kwong type EOS. [b] PT-SWP: perturbation type EOS with repulsion and an attraction term with square-well potential for intermolecular interaction. [c] RKJZ: Redlich−Kwong−Joffe−Zudkevitch type EOS. [d] PR: Peng−Robinson type EOS. [e] QCGCH: quasi-chemical group−contribution hole model.

5. Crossover Free-Energy Model

In this study, we have used the parametric crossover model CREOS-97 developed by Kiselev,[74] as modified later by Kiselev and Rainwater.[75,76] Although the CREOS-97 was initially developed for Type I mixtures only, as was demonstrated in our previous work (Kiselev et al.[77]) for water + toluene mixtures, it can also be applied to Type III mixtures. The crossover free-energy density in this model is given by

$$\rho\tilde{A}(T,\rho,\tilde{x}) = \rho A(T,\rho,x) - \rho\tilde{\mu}(T,\rho,x) \tag{3}$$

where $\tilde{\mu} = \mu_2 - \mu_1$ is the difference of the chemical potentials μ_1 and μ_2 of the mixture components, $x = N_2/(N_1 + N_2)$ is the mole fraction of the second component in the mixture, $\rho A(T,\rho,x)$ is the Helmholtz free-energy density of the mixture, and the isomorphic field variable $\tilde{x}$ is related to the chemical potential of the mixture $\tilde{\mu}$ by the relation

$$\tilde{x} = \frac{e^{\tilde{\mu}/RT}}{1 + e^{\tilde{\mu}/RT}} = 1 - \varsigma \tag{4}$$

where ς is a field variable first introduced by Griffiths and Wheeler.[78] The thermodynamic equation

$$x = -\tilde{x}(1-\tilde{x})\left(\frac{\partial\tilde{A}}{\partial\tilde{x}}\right)_{T,\rho}\frac{1}{RT} \tag{5}$$

(where R is the universal gas constant) provides a relation between the concentration x and the isomorphic variable $\tilde{x}$. Similar to the concentration, the isomorphic variable $\tilde{x}$ changes from 0 to 1 for $0 \le x \le 1$. At fixed $\tilde{x}$, the isomorphic free-energy $\rho\tilde{A}$ is the same function of T and ρ as the Helmholtz free-energy density of a one-component fluid[74,77,79−81]

$$\frac{\rho\tilde{A}(T,\rho,\tilde{x})}{RT_{c0}\rho_{c0}} = \tilde{k}r^{2-\alpha}\tilde{R}^{\alpha}(q)[\tilde{a}\Psi_0(\vartheta) + \sum_{i=1}^{5}\tilde{c}_i r^{\Delta_i}\tilde{R}^{-\tilde{\Delta}_i}(q)\Psi_i(\vartheta)] + \sum_{i=1}^{4}\left(\tilde{A}_i + \frac{\rho}{\rho_c(\tilde{x})}\tilde{m}_i\right)\tau^i(\tilde{x}) - \frac{P_c(\tilde{x})}{RT_{c0}\rho_{c0}} + \frac{\rho T}{T_{c0}\rho_{c0}}[\ln(1-\tilde{x}) + \tilde{m}_0] \tag{6}$$

$$\tau = \frac{T - T_c(\tilde{x})}{T_c(\tilde{x})} = r(1 - b^2\vartheta) \tag{7}$$

$$\Delta\rho = \frac{\rho - \rho_c(\tilde{x})}{\rho_c(\tilde{x})} = \tilde{k}r^{\beta}\tilde{R}^{-\beta+1/2}(q)\vartheta + \tilde{d}_1\tau \tag{8}$$

where b^2 is a universal linear-model parameter[74] and $\tilde{k}$, $\tilde{d}_1$, $\tilde{a}$, $\tilde{c}_i$, A_i, and m_i are the system-dependent coefficients. The crossover function $\tilde{R}(q)$ is defined by the expression[75]

$$\tilde{R}(q) = \left(1 + \frac{q^{2\Delta_0}}{1 + q^{\Delta_0}}\right)^{(1/\Delta_0)}, \quad q = r\tilde{g} \tag{9}$$

where $\tilde{g} \propto Gi^{-1}$ (here Gi is the Ginzburg number for fluid of interest[82−84]) and Δ_0 is a universal constant. The exact expressions for the universal scaled functions $\Psi_i(\vartheta)$ are given in Table 5.

In eqs 6−9, all nonuniversal parameters as well as the critical parameters $T_c(\tilde{x})$, $\rho_c(\tilde{x})$, and $P_c(\tilde{x})$ are analytical functions of the isomorphic variable $\tilde{x}$. In this work, following the previous studies[75,76,85−87] for Type I binary mixtures, we represent these functions, defined as $Y_c(\tilde{x})$, as simple polynomial forms of $\tilde{x}$ and $(1 - \tilde{x})$

$$Y_c(\tilde{x}) = Y_{c0}(1-\tilde{x}) + Y_{c1}\tilde{x} + (1-\tilde{x})\sum_{i=1} y_i\tilde{x}^i \tag{10}$$

where $Y_c \in \{T_c, P_c, \rho_c\}$ and the subscripts *c0* and *c1* correspond to the pure solvent (water) and solute (n-hexane), respectively. In addition to eq 10, we adopt a so-called critical line condition (CLC) in the form[74−76]

$$\frac{d\tilde{m}_0}{d\tilde{x}} = \frac{1}{RT_c\rho_c}\frac{dP_c}{d\tilde{x}} + (\tilde{A}_1 + \tilde{m}_1)\frac{\rho_{c0}}{\rho_c}\frac{T_{c0}}{T_c^2}\frac{dT_c}{d\tilde{x}} \tag{11}$$

which implies that a zero level of the entropy of a binary mixture can be chosen so that the isomorphic variable $\tilde{x} = x$ along the whole critical line, including the pure solvent limit.

To specify the crossover equation for $\tilde{A}(T,\rho,\tilde{x})$ of a binary mixture, we also need the system-dependent parameters $\tilde{d}_1(\tilde{x})$, $\tilde{k}(\tilde{x})$, $\tilde{a}(\tilde{x})$, $\tilde{c}_i(\tilde{x})$, $\tilde{m}_i(\tilde{x})$, and $\tilde{A}_i(\tilde{x})$ as functions of the isomorphic variable $\tilde{x}$. To represent all system-dependent parameters in eq 10, designated as $\tilde{k}_i(\tilde{x})$, as functions of $\tilde{x}$, we utilize the hypothesis (Kiselev et al.[88]) that, in binary mixtures, all system-dependent parameters depend on $\tilde{x}$ only through the excess critical compressibility factor $\Delta Z_c(\tilde{x})$, where

$$\Delta Z_c(\tilde{x}) = Z_c(\tilde{x}) - Z_{cid}(\tilde{x}) \tag{12}$$

is the difference between the actual compressibility factor of a mixture $Z_c(\tilde{x}) = P_c(\tilde{x})/R\rho_c(\tilde{x})T_c(\tilde{x})$ and its "ideal" part $Z_{cid}(\tilde{x}) = Z_{c0}(\tilde{x})(1 - \tilde{x}) - Z_{c1}\tilde{x}$. The dimen-

Table 5. Universal Scaled Functions

$$\Psi_0(\vartheta) = \frac{1}{2b^4}\left[\frac{2\beta(b^2-1)}{2-\alpha} + \frac{2\beta(2\gamma-1)}{\gamma(1-\alpha)}(1-b^2\vartheta^2) - \frac{(1-2\beta)}{\alpha}(1-b^2\vartheta^2)^2\right]$$

$$\Psi_1(\vartheta) = \frac{1}{2b^2(1-\alpha+\Delta_1)}\left[\frac{\gamma+\Delta_1}{2-\alpha+\Delta_1} - (1-2\beta)b^2\vartheta^2\right]$$

$$\Psi_2(\vartheta) = \frac{1}{2b^2(1-\alpha+\Delta_2)}\left[\frac{\gamma+\Delta_2}{2-\alpha+\Delta_2} - (1-2\beta)b^2\vartheta^2\right]$$

$$\Psi_3(\vartheta) = \vartheta - \frac{2}{3}(e_0-\beta)b^2\vartheta^3 + \frac{e_1(1-2\beta)}{(5-2e_0)}b^4\vartheta^5$$

$$\Psi_4(\vartheta) = \frac{1}{3}b^2\vartheta^3 - \frac{e_2(1-2\beta)}{(5-2e_0)}b^4\vartheta^5$$

$$\Psi_5(\vartheta) = \frac{1}{3}b^2\vartheta^3 - \frac{e_4(1-2\beta)}{(2e_3-5)}b^4\vartheta^5$$

sionless coefficients $\tilde{d}_1(\tilde{x})$ and $\tilde{k}(\tilde{x})$ are written in the form[74,75]

$$\tilde{k}_i(\tilde{x}) = k_{i0} + (k_{i1}-k_{i0})\tilde{x} + k_i^{(1)}\Delta Z_c(\tilde{x}) + k_i^{(2)}\Delta Z_c(\tilde{x})^2 \quad (13)$$

and all other coefficients are given by

$$\tilde{k}_i(\tilde{x}) = \frac{P_c(\tilde{x})}{R\rho_c(\tilde{x})T_c(\tilde{x})}[k_{i0} + (k_{i1}-k_{i0})\tilde{x} + k_i^{(1)}\Delta Z_c(\tilde{x}) + k_i^{(2)}\Delta Z_c(\tilde{x})^2] \quad (14)$$

Within the law of corresponding states (LCS), the mixing coefficients $k_i^{(j)}$ in eqs 13 and 14 are universal constants for all binary mixtures with $\Delta Z_c \leq 0.2$ (Kiselev and Rainwater[75]).

The parametric crossover model for binary mixtures is specified by eqs 6−14 and contains the following universal constants: the critical exponents α, β, Δ_i, $\tilde{\Delta}_i$, and the linear-model parameter b^2. The values of all universal constants are listed in Table 6.

To use the parametric crossover model defined by eqs 6−9, together with eqs 13 and 14, one needs to know first the system-dependent coefficients k, d_1, a, c_i, g, A_i, and m_i for pure components ($\tilde{x} = 0$ and $\tilde{x} = 1$). For pure water ($\tilde{x} = 0$), we adopted the critical parameters T_{c0}, ρ_{c0}, and P_{c0}, and coefficients k_0, d_{10}, a_0, c_{i0}, g_0, A_{i0}, and m_{i0} as reported by Kiselev and Friend[89] and used earlier by Kiselev et al.[77] for water + toluene mixtures. For pure n-hexane ($\tilde{x} = 1$), the critical parameters T_{c1}, ρ_{c1}, and P_{c1}, and the coefficients k_1, d_{11}, a_1, c_{i1}, g_1, A_{i1}, and m_{i1} were found from a fit of eqs 6−9 to the *PVT* data sets by Kurumov and Grigorev[90,91] and by Abdulagatov et al.[58] together with isochoric heat capacity data of Amirkhanov et al.[92] We did this in two steps. First, we optimized eqs 6−9 to the experimental data in the near critical region at $\tau + 1.2\Delta\rho^2 \leq 0.1$. In the second step, the coefficients d_{11}, c_{i1} ($i > 1$), g_1, A_{i1}, and m_{i1} have been redefined from a fit of the crossover equation of state, with the fixed values of the critical parameters and coefficients k_1, a_1, and c_{11}, to the experimental *PVTx* and C_V data in the range of temperatures and densities bounded by

$$\tau + 1.2\Delta\rho^2 \leq 0.5,\ T \geq 0.98T_c \quad (15)$$

This range of validity of the parametric crossover model is the same as reported earlier by Kiselev and Friend[89] for pure water. The values of all system-dependent coefficients for pure components and their mixtures are listed in Tables 7 and 8.

To specify the crossover free-energy density model for a binary mixture, one needs also to know the critical locus for the mixture. In this work, for the critical locus in dilute H_2O + n-C_6H_{14} mixtures, we used eq 10, where the coefficients $y_i \in \{t_i, p_i\}$ for T_c and P_c were found from a fit of eq 10 to the experimental $T_c(x)$ and $P_c(x)$ data listed in Table 2. Comparisons of the critical locus data with values calculated with eqs 10 are shown in Figures 4a−c and 5. As one can see, for $P_c - T_c$, $T_c(x)$, and $P_c(x)$ loci good agreement between experimental data and calculated values is observed. We are not aware of experimental $\rho_c(x)$ data for dilute aqueous n-hexane solution; therefore, for the coefficients y_i in eq 10 for the critical density we found from a fit of the parametric crossover model as given by eqs 6−14 to the present experimental *PVTx*. The different curves in Figure 4c represent the values calculated with eq 10 with different sets of the parameters ρ_i obtained from different fits to experimental *PVTx* data. As one can see from Figure 4c, at compositions $x \leq 0.03$ mole fraction of n-hexane, where the most experimental data have been obtained, all curves practically coincide. However, at $x > 0.03$, the difference between the critical densities calculated with different sets of the parameters ρ_i increases drastically. As a consequence, the difference between the critical compressibility factor Z_c and the excess compressibility ΔZ_c calculated with these critical densities are also increased dramatically (see Figure 6). We do not know which of the curves presented in Figures 4c and 6 is correct; therefore, in this work we have chosen the simplest set of the parameters ρ_i, which are shown in Figures 4c and 6 by the solid curves. The values of the critical-locus parameters $y_i \in \{t_i, p_i, \rho_i\}$ in eq 10 are listed in Table 8.

6. Results and Discussion

6.1. Pure *n*-Hexane. To check and confirm the quality and predictive capability of the crossover model, we made a comprehensive comparison of the present crossover EOS for pure n-hexane with the available experimental data in the critical and supercritical regions. In particular, we made a detailed comparison

Table 6. Universal Constants

$\alpha = 0.110$
$\beta = 0.325$
$\gamma = 2 - \alpha - 2\beta = 1.24$
$b^2 = (\lambda - 2\beta)/\gamma(1-2\beta) \cong 1.359$
$\Delta_1 = \tilde{\Delta}_1 = 0.51$
$\Delta_2 = \tilde{\Delta}_2 = 2\Delta_1 = 1.02$
$\Delta_3 = \Delta_4 = \gamma + \beta - 1 = 0.565$
$\Delta_5 = 1.19$
$\tilde{\Delta}_3 = \tilde{\Delta}_4 = \Delta_3 - 0.5 = 0.065$
$\tilde{\Delta}_5 = \Delta_5 - 0.5 = 0.69$
$e_0 = 2\gamma + 3\beta - 1 = 2.455$
$e_1 = (5-2e_0)(e_0-\beta)(2e_0-3)/3(e_0-5\beta) \cong 0.147$
$e_2 = (5-2e_0)(e_0-3\beta)/3(e_0-5\beta) \cong 5.35 \times 10^{-2}$
$e_3 = 2 - \alpha - \Delta_5 = 3.08$
$e_4 = (2e_3-5)(e_3-3\beta)/3(e_3-5\beta) \cong 0.559$
$\Delta_0 = 0.5$

Table 7. Mixture Coefficients

parameter	water (k_{i0})	n-hexane (k_{i1})	$k_i^{(1)}$	$k_i^{(2)}$
		Critical Amplitudes		
k	1.41380	1.13977	−4.1776	4.1893
d_1	-7.13319×10^{-1}	-9.22176×10^{-1}	0.5862	1.9908×10
a	2.25383×10	2.643562×10	-1.4994×10	-6.6113×10
c_1	−6.83712	-2.58869×10	-6.7479×10	1.9677×10^2
c_2	1.33215×10	5.87390×10	0	0
c_3	-1.16219×10	-1.34410×10	−2.2191	-2.4752×10^2
c_4	7.83568	1.35784×10	2.2675×10	2.5603×10^2
		Crossover Parameter		
g	1.80152×10^{-5}	2.08137	−4.0512	3.0924×10^2
		Background Coefficients		
A_1	−7.81074	−7.60374	6.6065	8.2305
A_2	1.81122×10	2.33107×10	-5.2671×10	2.4531×10
A_3	2.72022	2.38793×10	0	0
m_1	0	−1.7911	2.8041	−2.5439
m_2	-1.14168×10	-5.36400×10	3.4528×10	0
m_3	6.23749	8.63509	-1.0180×10	0
m_4	−6.41886	0	0	0
		Molecular Weight		
M_W	18.0152	8.61780E+01	0	0

Table 8. Critical Parameters for Dilute H_2O + n-C_6H_{14} Solutions

			Pure Water		
P_{c0}, MPa	22.064	T_{c0}, K	647.096	ρ_{c0}, mol·L^{-1}	17.874
			Mixture Coefficients		
p_1, MPa	1.20916757×10^5	t_1, K	2.08728461×10^4	ρ_1, mol·L^{-1}	1.32285674×10^4
p_2, MPa	-3.85848892×10^5	t_2, K	-4.50143038×10^4	ρ_2, mol·L^{-1}	3.28792339×10^4
p_3, MPa	4.11578554×10^5	t_3, K	2.39457775×10^4	ρ_3, mol·L^{-1}	2.42767881×10^4
p_4, MPa	-1.46662825×10^5			ρ_4, mol·L^{-1}	4.59179121×10^3
			Pure n-Hexane		
P_{c1}, MPa	3.088	T_{c1}, K	507.790	ρ_{c1}, mol·l^{-1}	2.6900

with experimental data for the *PVT*, isobaric and isochoric heat capacity data. Table 9 provides the deviation statistics for these data.[97] In the range of the densities and temperatures given by eq 15, the deviations between experimental density data and values calculated with crossover EOS are to within 0.5%, which approximately corresponds to the accuracy achieved with other multiparametric analytical type equation of state by Span,[93] Polt et al.,[94] Starling,[95] and Grigor'ev et al.[96,97] Some of these EOS are directly fitted to various properties as *PVT*, C_P, speed of sound data W, and saturation properties (P_S,ρ_S',ρ_S); therefore, it can be expected to reproduce some properties as well as the crossover EOS which is not fitted directly to these data. However, all these analytical equations fail to reproduce nonanalytical singular behavior of the isochoric heat capacity in the critical region.

Figure 7 shows the results of the isochoric heat capacity calculations with present crossover EOS together with experimental values reported by Amirkhanov et al.[92] and the values calculated from multiparametric analytical EOS along the critical isochore in the one- and two-phase regions. As can be seen from Figure 7, in the one-phase region at the temperature above 553 K all calculations are in good agreement with experi-

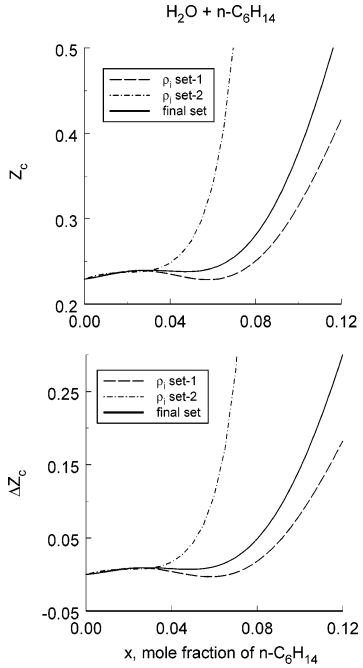

Figure 6. Critical compressibility Z_c (top) and excess critical compressibility ΔZ_c (bottom) for dilute H_2O + n-C_6H_{14} solutions as a function of composition calculated with eq 10.

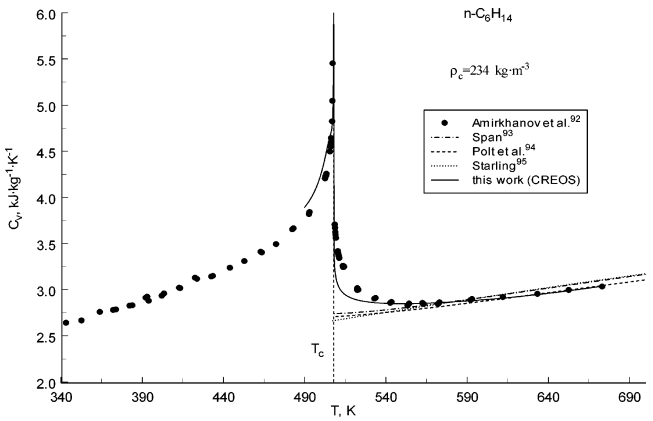

Figure 7. One- and two-phase isochoric heat capacities of the pure n-hexane as a function of temperature along the critical isochore.

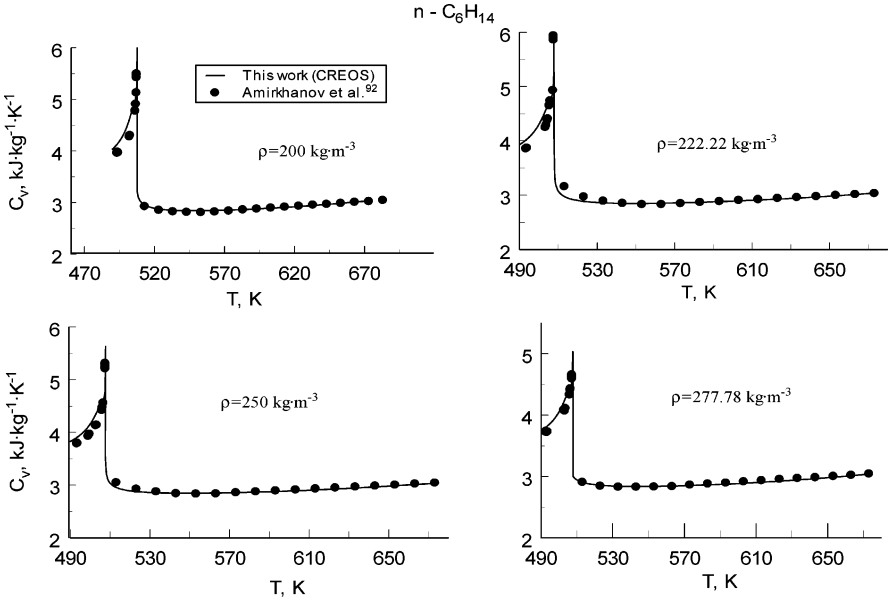

Figure 8. One- and two-phase isochoric heat capacities of the pure n-C_6H_{14} as a function of temperature along the sub- (left) and supercritical (right) isochores.

mental data (deviations are about 1−2%), while near the critical point (about 45−50 K from the critical temperature) analytical equations fail to reproduce the anomalous behavior of the C_V in the critical region. Similar behavior was found along the other near critical isochores close to the phase transition temperatures (see Figure 8). As one can see, in contrast to analytical EOS, the present crossover model is able to represent the C_V data to within their experimental uncertainty in the critical and supercritical regions and near the phase transition curve.

Figure 9 shows comparisons of the enthalpy data reported by Wormald and Yerlett[99] for pure n-hexane at sub- and supercritical regions with the values calculated from the present crossover model. The excellent agreement within 0.56% is observed at pressures above P_C and in the vapor phase near the phase transition curve. Deviation statistics are as follows: AAD = 0.56%; Bias = 0.18%; St.Dev = 0.70%; St.Err = 0.09%; MaxDev = 1.8%; N = 80. Maximum deviations up to 2−4% were found in the critical region (along a near critical isotherm of 510.2 K and pressures between 3 and 3.5 MPa). Extrapolation to low pressures (to the vapor phase) shows the deviations within 6−9%.

To show how the crossover model represents other thermodynamic properies at saturation near the critical point, a comparison with selected relaiable experimental data are given in Figures 10−12. These figures provide a comparison of the present calculated values of the various thermodynamic properties (P_S,ρ_S',ρ_S,C_{Ps}') of pure n-hexane on the saturated curve with available

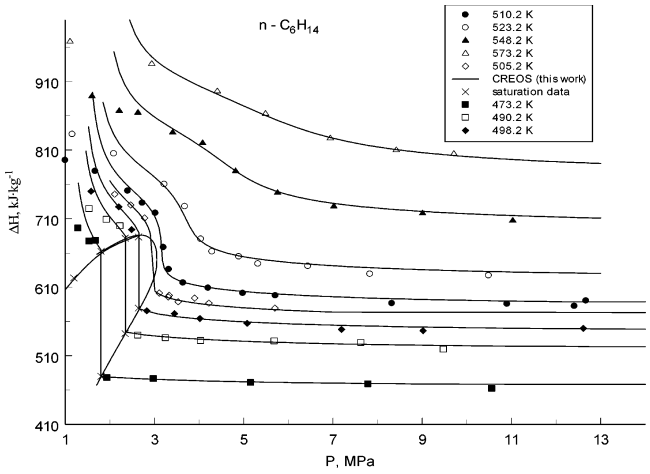

Figure 9. Enthalpy of the pure n-C_6H_{14} as a function of pressure in the sub- and supercritical regions. The symbols indicate experimental data reported by Wormald and Yerlett.[99] The solid curves represent values calculated from present crossover model.

experimental data. No saturated properties data were used in the determination of any of the system-dependent constants in the present crossover equation for n-hexane. AAD for the saturation data are as follows: vapor pressure, 0.13%; saturated density data, 0.47%; saturated isochoric heat capacity data, 2−4%; saturated isobaric heat capacity data, 3−4%; speed of sound data at saturation, 1−2%; and saturated enthalpy data, 0.21%. The present crossover model correctly represents all of the availably saturation data near the critical

Table 9. Deviation Statistics for Thermodynamics Properties of Pure n-Hexane

	PVT, Kurumov and Grigor'ev[90,91]	PVT, Abdulagatov et al.[58]			C_V, Amirkhanov et al.[92]			C_P, Gerasimov et al.[98]
deviations	CREOS this work	CREOS this work	Span[93]	Starling[95]	CREOS this work	Span[93]	Starling[95]	CREOS this work
AAD, %	0.22	0.45	0.54	0.60	0.52	1.64	1.72	1.30
BIAS, %	0.01	0.31	−0.45	−0.20	−0.13	−0.12	−0.34	−0.72
SDV, %	0.34	0.47	0.72	0.88	0.73	2.11	0.95	1.29
RMS, %	0.02	0.11	0.12	0.18	0.04	0.10	0.15	0.16
MAXDEV,%	1.25	1.36	−1.28	2.0	3.5	5.98	5.12	3.80
N	300	30	30	30	300	431	431	100

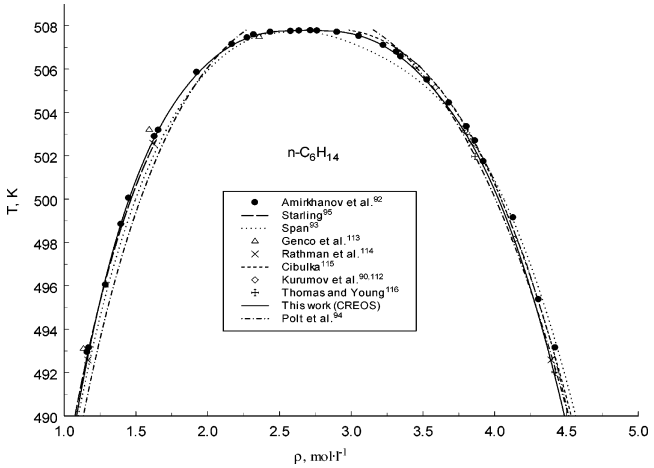

Figure 10. Vapor−liquid coexistence curves of pure n-C_6H_{14} calculated with present crossover model together with experimental data reported by other authors from the literature.

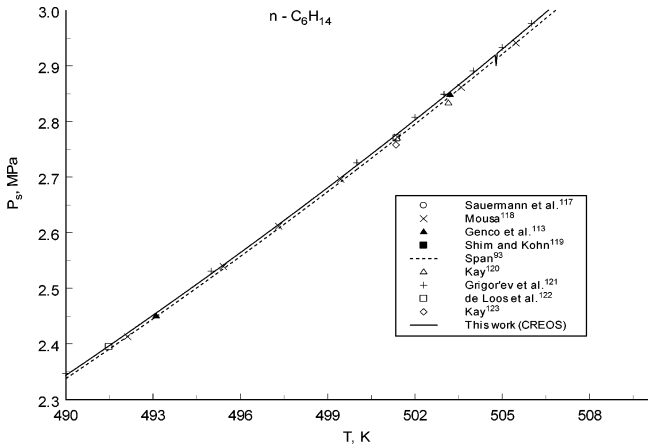

Figure 11. Vapor-pressure curves of pure n-C_6H_{14} near the critical point calculated with present crossover model together with experimental data reported by other authors from the literature.

point to within their experimental uncertainties without systematic deviations. This excellent agreement confirms the reliability and accuracy of the present crossover model and correct representation all of the typical thermodynamic anomalous behavior of the near- and supercritical fluids.

6.2. Dilute Aqueous *n*-Hexane Solutions. Measurements of the *PVTx* relationship of the aqueous *n*-hexane solutions were carried out at three compositions (0.0201, 0.0850, and 0.8500 mole fraction of *n*-hexane) for the critical isotherm of pure water 647.1 K. The density ranged from 39 to 492 kg·m^{-3}, and the pressure ranged from 8 to 33 MPa. The experimental *PVTx* and compressibility factor results are presented

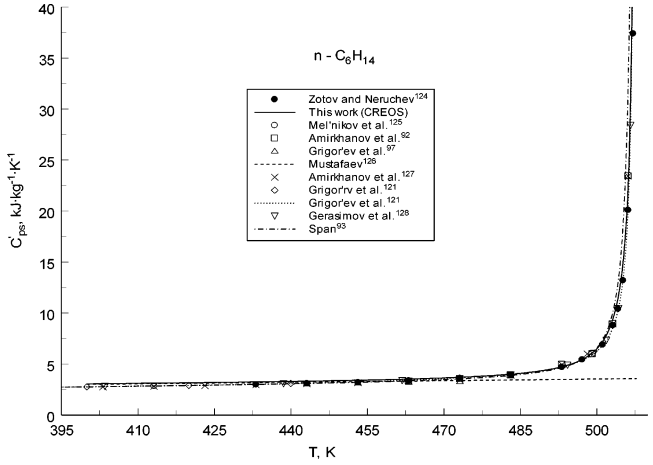

Figure 12. Isobaric heat capacity of pure n-C_6H_{14} at saturation near the critical point calculated with present crossover model together with experimental data reported by other authors from the literature.

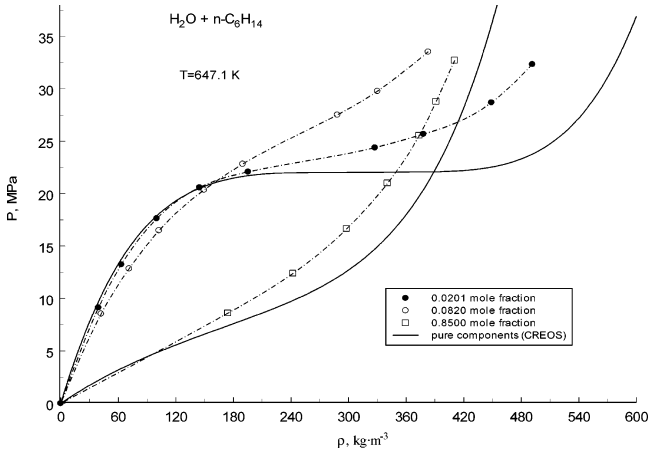

Figure 13. Measured pressures P of H_2O + n-hexane mixtures as a function of density ρ along the critical isotherm of pure water for various compositions together with values for pure components.

in Table 10. Some selected experimental results are shown in Figures 13−15 as projections in the $P-\rho$, $Z-P$, and $P-x$ planes, together with values calculated from IAPWS[67] for pure water and pure n-C_6H_{14} calculated with Span.[93] Figure 15 includes also our previous measurements (Abdulagatov et al.[35]).

Measured values of pressure P as a function of composition x along the solvent's critical isotherm-isochore (pure water) (T_C = 647.1 K and ρ_C = 322.0 kg·m^{-3}, see Figure 15) can be used to determine the value of the Krichevskii parameter $(\partial P/\partial x)^{\infty}_{T_cV_c}$ as the slope of the experimental $P-x$ curve at $x \rightarrow 0$. Our experimental result for $(\partial P/\partial x)^{\infty}_{T_cV_c}$ is 124.4 ± 20 MPa

Table 10. Experimental $P\rho Tx$ Data for H_2O + *n*-Hexane along the Critical Isotherm of Pure Water

T = 647.10 K								
x = 0.0201 mole fraction n-C_6H_{14}			x = 0.082 mole fraction n-C_6H_{14}			x = 0.850 mole fraction n-C_6H_{14}		
ρ (kg·m^{-3})	P (MPa)	Z	ρ (kg·m^{-3})	P (MPa)	Z	ρ (kg·m^{-3})	P (MPa)	Z
39.320	9.140	0.8377	42.120	8.550	0.8904	174.24	8.610	0.6976
63.140	13.25	0.7563	71.250	12.85	0.7911	242.18	12.40	0.7228
100.12	17.63	0.6346	102.41	16.49	0.7063	297.90	16.64	0.7885
144.62	20.60	0.5133	149.33	20.35	0.5978	340.58	21.00	0.8704
195.37	22.09	0.4075	189.74	22.83	0.5278	373.65	25.55	0.9653
327.49	24.40	0.2685	288.35	27.52	0.4186	391.33	28.80	1.0389
378.14	25.69	0.2448	330.09	29.78	0.3957	410.61	32.71	1.1245
448.95	28.69	0.2303	383.00	33.53	0.3840			
491.62	32.34	0.2371						

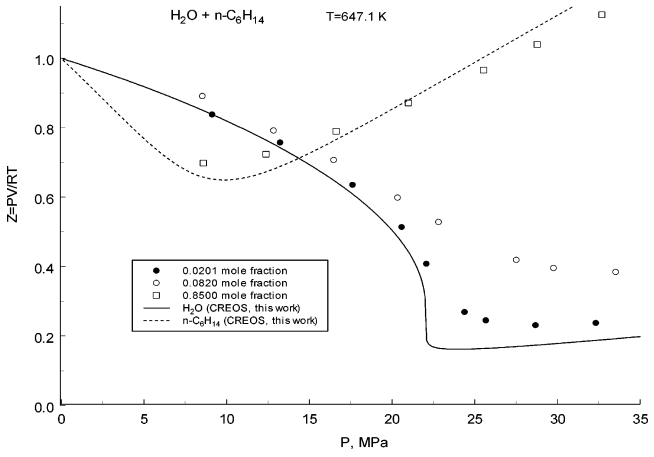

Figure 14. Measured compressibility factors $Z = PV/RT$ of $H_2O + n\text{-}C_6H_{14}$ mixtures as a function of pressure P along the critical isotherm of pure water for various compositions together with values for pure components.

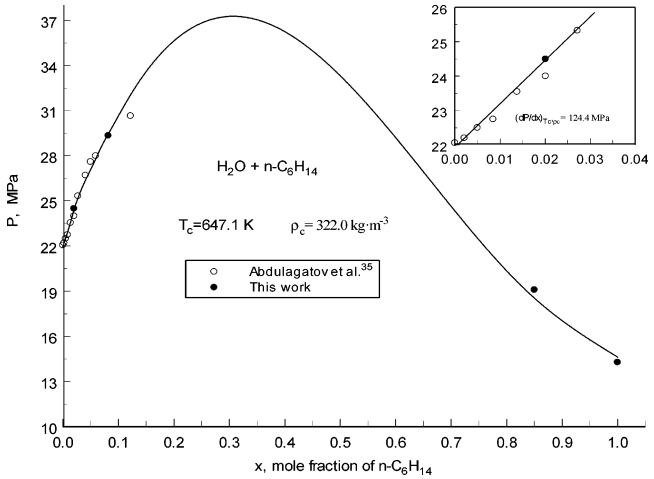

Figure 15. Measured pressures P of $H_2O + n\text{-}C_6H_{14}$ mixtures as a function of composition x along the critical isotherm-isochore of pure water.

and the value calculated with the crossover model is 119.54 MPa, which is in excellent agreement with the value of the Krichevskii parameter obtained earlier by Abdulagatov et al.[102] (119 MPa) from the analysis of the critical locus data. The Krichevskii parameter in dilute aqueous *n*-hexane solutions has also been studied recently by Plyasunov et al.[100,101] The values reported by Plyasunov et al.[100,101] (168 and 197 ± 40 MPa) are about 30−40% bigger than the ones obtained in the present work.

Figures 16−19 compare the present and our previous (Abdulagatov et al.[35]) *PVTx* data with the values calculated with the crossover model. As one can see, good agreement (within 0.36%) is observed between our previous measurements (Abdulagatyov et al.[35]) and values calculated with the crossover model. An agreement between present data and the values calculated with the crossover model is fairly good (within 0.5%) up to the densities 525 kg·m^{-3}. It should be emphasized that none of the experimental data shown in Figures 16−19 have been used for the optimization of the crossover model. Therefore, the obtained results look rather impressive.

Figure 18 compares our previous density measurements and the data reported by Degrange[36] for infinite dilution $H_2O + n\text{-}C_6H_{14}$ mixture at a pressure of 28.1

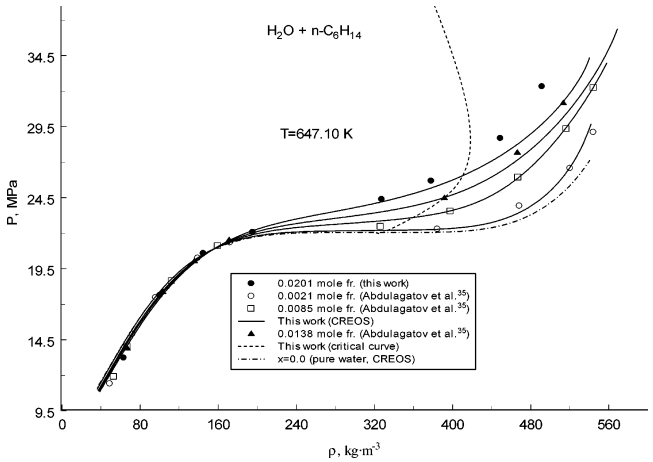

Figure 16. Measured pressures P as a function of density ρ for a $H_2O + n\text{-}C_6H_{14}$ mixture along the critical isotherm of pure water for various compositions together with values calculated from present crossover model.

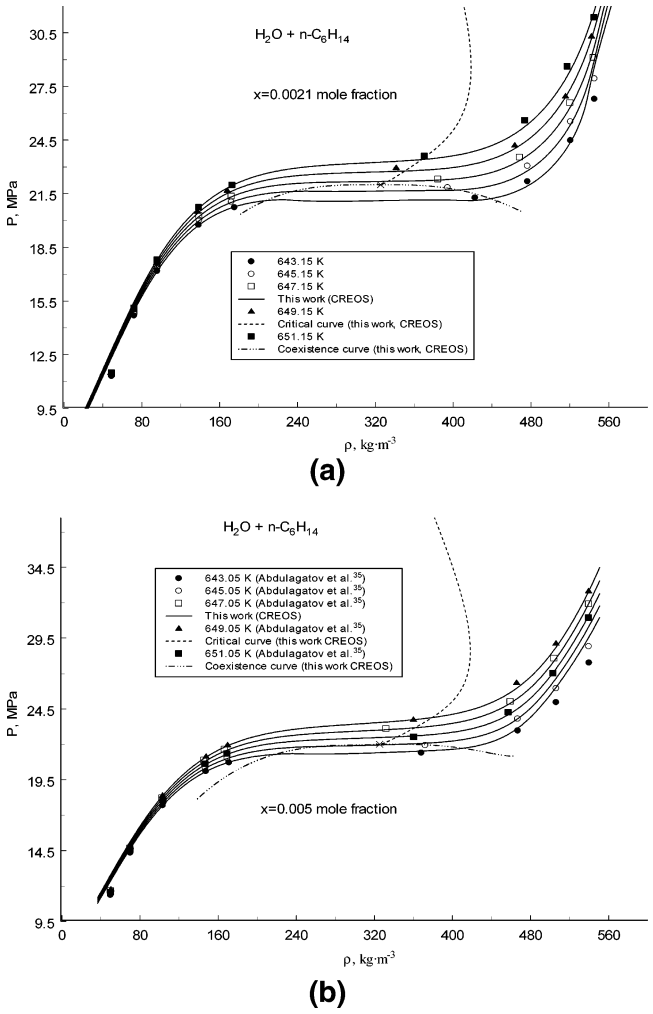

Figure 17. (a,b) Measured pressures P as a function of density ρ along various near-critical and supercritical isotherms for a $H_2O + n\text{-}C_6H_{14}$ mixture at concentrations of 0.0201 and 0.005 mole fraction of *n*-hexane together with values calculated from present crossover model.

MPa with the values calculated from the crossover model. Excellent agreement (within ±0.15% and 0.13%) between the values calculated with the crossover model and experimental data by Abdulagatov et al.[35] and by Degrange[36] is observed. Figure 19 shows the concentra-

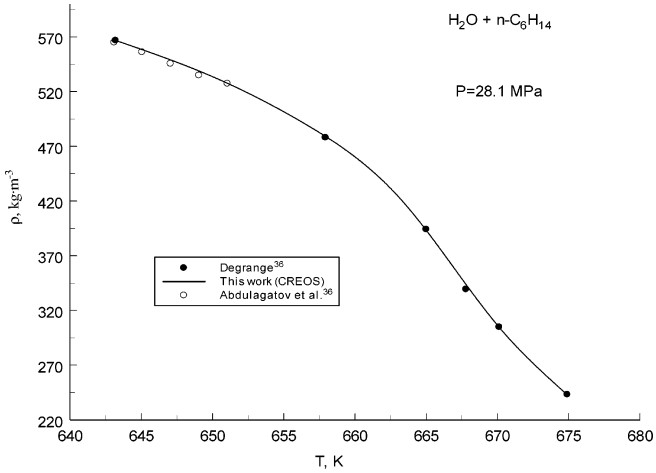

Figure 18. Measured densities ρ of infinite dilution H_2O + n-C_6H_{14} mixtures as a function of temperature along supercritical isobar of pure water 28.1 MPa together with values calculated from present crossover model.

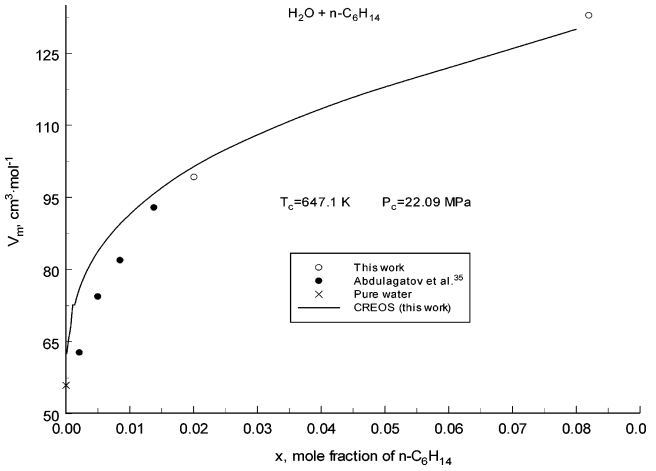

Figure 19. Measured molar volumes V_m as a function of composition x along the solvent's (water) critical isotherm-isobar for H_2O + n-C_6H_{14} mixtures together with values calculated from present crossover model.

tion dependence of the experimental molar volumes of H_2O + n-C_6H_{14} mixtures along critical isotherm-isobar of pure water together with the values calculated with the crossover model. As one can see from Figure 19, in the limit $x \to 0$ the tangent (slope of the V_m–x curve along the solvent's critical isotherm-isobar) approaches the vertical line and, therefore, the values of the derivative $(\partial V/\partial x)^{\infty}_{P_cT_c}$ dominate in the partial molar volume. Since the partial molar volume $\bar{V}_2^{\infty}$ of solute (n-C_6H_{14}) is obtained from the tangent $(\partial V_m/\partial x)^{\infty}_{PT}$

$$\bar{V}_2 = V_m + (1 - x)\left(\frac{\partial V_m}{\partial x}\right)_{PT} \tag{16}$$

the partial molar volume of infinitely dilute system near the critical point of pure water tends to plus infinity $\bar{V}_2^{\infty} \to +\infty$. In the limit of infinite dilution we have

$$\lim_{x\to 0}\left(\frac{\partial \ln V_m}{\partial x}\right) = K_{T,x}\lim_{x\to 0}\left(\frac{\partial P}{\partial x}\right)_{TV} \tag{17}$$

and since Krichevskii function does not diverge at the solvent's critical point, the partial molar volume can also

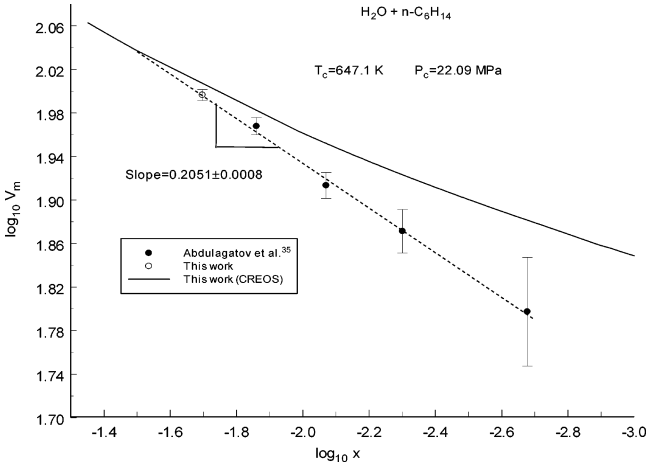

Figure 20. Molar volume $\log_{10} V_m$ against concentration $\log_{10} x$ for H_2O + n-C_6H_{14} mixtures along the pure solvent's (water) critical isotherm-isobar in the asymptotic region.

be calculated using concentration derivatives of pressure $(\partial P/\partial x)^{\infty}_{T_cV_c}$ as

$$\bar{V}_2^{\infty} = \rho^{-1}\left[K_T\left(\frac{\partial P}{\partial x}\right)_{TV}^{\infty} + 1\right] \tag{18}$$

where K_T is the compressibility of pure solvent (water), which strongly diverges at the critical point of the solvent as $K_T \propto (T - T_C)^{-\gamma} \to +\infty$, and ρ is the density of pure solvent (water). Therefore, the partial molar volume $\bar{V}_2^{\infty}$ will also diverge strongly at the solvent's critical point. The sign of the divergence depends on the values of $\mathrm{Lim}_{X\to 0}[(\partial P/\partial x)_{VT}]$ ($K_T > 0$ and values of the $K_T(\partial P/\partial x)^{\infty}_{TV} \gg 1$ near the critical point). The critical anomaly of the partial molar volume $\bar{V}_2^{\infty}$ is caused by the critical effects due to the divergence of the isothermal compressibility K_T of the pure solvent (water) and is common to all dilute near-critical mixtures. According to scaling theory of infinity dilution solutions, $\bar{V}_2^{\infty}$ along the solvent's critical isotherm-isobar diverges as $x^{-\epsilon}$ with the critical exponent $\epsilon = \gamma/\beta\delta$ (Levelt-Sengeres et al.[21]). Figure 20 shows experimental $\log_{10} V_m$ as a function of $\log_{10} x$ for H_2O + n-C_6H_{14} mixture along the critical isotherm-isobar of pure solvent (water). In this work, from a fit of the correlation $\log_{10} V_m = \log_{10} V_0 + (1 - \epsilon)\log_{10} x$ to the experimental data we found that in dilute aqueous n-hexane solutions the critical exponent $\epsilon = 0.795 \pm 0.002$, which is very close to the nonclassical value $\epsilon = 0.790$ (with $\gamma = 1.25$, $\beta = 0.325$, and $\delta = (\gamma + 1)/\beta \cong 4.82$), which differs from the classical, or mean-field, value $\epsilon_{mf} = 0.5$ ($\gamma_{\mathrm{mf}} = 1$, $\beta_{\mathrm{mf}} = 0.5$, and $\delta_{\mathrm{mf}} = 4$).

A data set of partial molar volumes at infinite dilution $\bar{V}_2^{\infty}$ was established for H_2O + n-C_6H_{14}, H_2O + benzene, and H_2O + toluene mixtures at temperatures up to 623 K and at pressures to 30 MPa by Majer et al.[57] They recommended the following correlation equation

$$\bar{V}_2^{\infty} = V_w + RTK_T\rho_W[a_1 + a_2(\exp(5\rho_W) - 1) + a_3\exp(1500/T)] \tag{19}$$

which describes the partial molar volume of a solute (n-hexane, benzene, and toluene) as a function of temperature T, density ρ_W, and compressibility K_T of pure water, a_1, a_2, and a_3 are the system-dependent parameters which were found from the experimental values of partial molar volume of hydrocarbon in infinitely dilute H_2O + hydrocarbon mixtures. In Figure 21, the

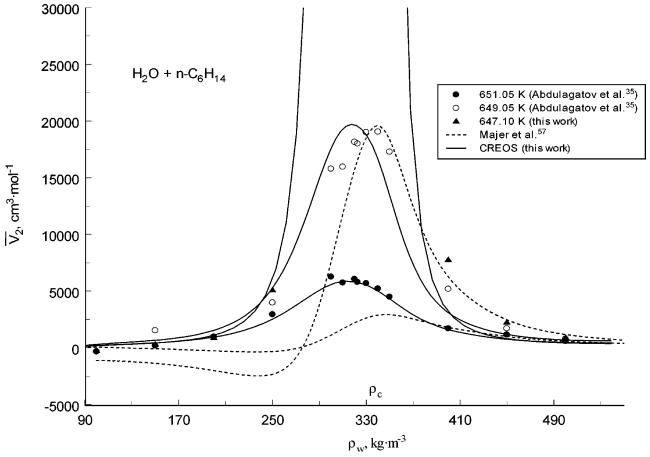

Figure 21. Comparison of the partial molar volume, $\bar{V}_2^{\infty}$, in the H_2O + n-C_6H_{14} mixture calculated with the present crossover model and semiempirical equation by Majer et al.[57] along the near-critical and supercritical isotherms with present experimental values.

partial molar volumes of n-C_6H_{14}, derived from our present and previous *PVTx* measurements and values calculated from eq 19 and the crossover model are shown as a function of pure solvent's (water) density ρ_W along the various near-critical and supercritical isotherms. Agreement between experimental values of the partial molar volumes $\bar{V}_2^{\infty}$ and those calculated with eq 19 is satisfactorily. Equation 19 is valid only up to 623 K.[57] Therefore, in Figure 21 the calculated values of $\bar{V}_2^{\infty}$ correspond to extrapolation of eq 19 to high temperatures. Far from the critical region (at densities lower than 250 kg·m^{-3} and higher than 410 kg·m^{-3}), the agreement between estimates made with eq 19 and values calculated with the crossover model is good. In the critical region, the systematic deviations between these two models are observed, which partially can be explained by the difference in the critical density in crossover model and in the semiempirical eq 19 used by Majer et al.[57] The partial molar volume calculated with eq 19 exhibits a maximum at a density of about 335 kg·m^{-3}, which is slightly higher than the critical density of pure water ($\rho_c^{H_2O}$ = 322.0 kg·m^{-3}) adopted by IAPWS[67] and in the crossover model. But in general, these deviations resulted from the analytical nature of eq 19. As one can see from Figure 21, the partial molar volume at infinite dilution at the critical point of pure water is positively diverging, which in principle cannot be described by analytical eq 19

Figures 22 and 23 show the values of excess enthalpy and isochoric heat capacity of dilute H_2O + n-C_6H_{14} mixtures in the supercritical region along the 657.92 K isotherm for the various compositions. Figure 22 also includes the single data point measured by Degrange[36] for a dilute H_2O + n-C_6H_{14} mixture at the same temperature and a pressure of 28.1 MPa. Figure 23 shows the behavior of $C_{V,x}$ as a function of $\log_{10}(T/T_C(x) - 1)$ along the critical isochores for various compositions. According to the principle of critical-point universality,[78,103,104] also called the isomorphism principle,[105,106] critical binary mixtures exhibit pure-fluid-like behavior at fixed chemical potential of binary mixture $\tilde{\mu}$, rather than composition x. As a consequence, the asymptotic behavior of the heat capacities $C_{V,x}$ and $C_{P,x}$ near the critical point in binary mixtures differs from the asymptotic behavior of C_V and C_P in pure fluids. An asymptotic behavior of the isochoric $C_{V,x}$ and

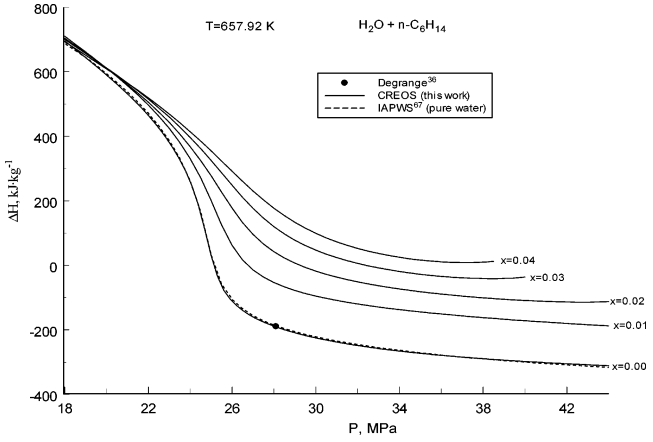

Figure 22. Excess enthalpies of H_2O + n-C_6H_{14} mixtures as a function of pressure along the supercritical isotherm of 657.92 K for various compositions.

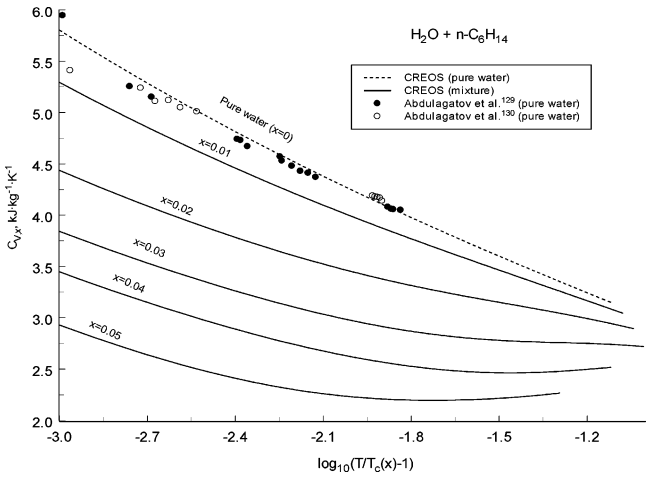

Figure 23. Isochoric heat capacity $C_{V,x}$ of the dilute H_2O + n-C_6H_{14} mixtures at $\rho = \rho_C(x)$ as a function of $\log_{10}(T/T_C(x) - 1)$ together with values calculated for pure water.

isobaric heat capacities $C_{P,x}$ along the critical isochore $\rho = \rho_c(x)$ in binary mixtures is determined by two characteristic temperatures[79,105−108]

$$\tau_\alpha(x) \cong \left[A_0 x(1-x)\left(\frac{1}{T_c}\frac{dT_c}{dx}\right)^2\right]^{1/\alpha} \tag{20}$$

and

$$\tau_\gamma(x) \cong \left[\Gamma_0 x(1-x)\left(\frac{1}{R\rho_c T_c}\frac{dP_{cxs}}{dx}\right)^2\right]^{1/\gamma} \tag{21}$$

where A_0 and Γ_0 are the critical amplitudes and the derivative dP_{cxs}/dx is taken along the two-phase coexistence boundary. In dilute solution limit, this derivative reduces to the Krichevskii parameter K_{kr}

$$K_{kr} = \lim(\partial P/\partial x)_{VTC} = \frac{dP_C}{dx} - (\partial P/\partial T)_{\xi,\rho=\rho_C}\frac{dT_C}{dx} \tag{22}$$

At temperatures $\tau_\gamma(x) \ll \tau \ll 1$, $C_{V,x}$ and $C_{P,x}$ exhibit pure-fluid-like singular behavior

$$\frac{C_{V,x}}{R} \approx A_0\tau(x)^{-\alpha} + Const \text{ and } \frac{C_{P,x}}{R} \approx \Gamma_0\tau(x)^{-\gamma} + Const \tag{23}$$

In the temperature range $\tau_\alpha(x) \ll \tau \ll \tau_\gamma(x)$, the isobaric heat capacity $C_{P,x}$ does not depend on temperature, $C_{P,x} \approx Const$, while the isochoric heat capacity $C_{V,x}$ demonstrates pure-fluid scaling law behavior as given by eq 23. Finally, asymptotically close to the critical point, such that $\tau \ll \tau_\alpha(x)$, the so-called Fisher renormalization[103] of the critical exponents $\alpha \rightarrow -\alpha/(1-\alpha)$ and $\gamma \rightarrow \alpha/(1-\alpha)$ takes place, and the heat capacities exhibit mixture-like singular behavior:

$$C_{V,x} \approx Const - \tau(x)^{\alpha/(1-\alpha)} \text{ and } C_{P,x} \approx \tau(x)^{-(\alpha/(1-\alpha))} + Const \quad (24)$$

At a concentration of $x = 0.06103$ mole fraction of *n*-hexane, the derivative $(dT_C/dx) = 0$ and, as a consequence, the parameter τ_α is equal to zero (see Figure 4a). At compositions $x \neq 0.06103$ and $x < 0.08$, the derivative $dT_c/dx \neq 0$, but it is small. Therefore, the values of $\tau_\alpha(x)$ are almost zero ($\tau_\alpha(x) \approx 10^{-9}-10^{-14}$), and the renormalization as given by eq 24 does not occur. In the entire experimentally available temperature region at $x < 0.08$ the $C_{V,x}$ exhibits a pure fluidlike behavior, as was shown in Figure 23. On the other hand, at concentrations $x > 0.08$ mole fraction of *n*-hexane, the parameter $\tau_\alpha(x)$ is not small anymore and the Fisher renormalization of $C_{V,x}$, as given by eq 24, should be observed in this mixture. Unfortunately, Kamilov et al.[39] measured $C_{V,x}$ for these mixtures at compositions which are out of the range where the renormalization of the critical behavior of $C_{V,x}$ can be observed. Therefore, to experimentally test the renormalization of the critical behavior of $C_{V,x}$ in $H_2O + n\text{-}C_6H_{14}$ mixtures, additional measurements in the concentration range from 0.084 to 0.12 mole fraction of *n*-hexane are needed.

7. Conclusions

The *PVTx* relationship of the three $H_2O + n\text{-}C_6H_{14}$ mixtures (0.0201, 0.0820, and 0.8500 mole fraction of *n*-hexane) were measured with a constant-volume piezometer immersed in a precision liquid thermostat. Measurements were made along the critical isotherm of pure water 647.1 K for the densities from 39 to 492 $kg \cdot m^{-3}$ with pressures between 8 and 33 MPa. The total uncertainty of density, pressure, temperature, and concentration measurements was estimated to be less than 0.16%, 0.05%, 15 mK, and 0.001 mole fraction of *n*-hexane, respectively. The Krichevskii parameter (124.4 ± 20 MPa) was derived using measured values of pressure *P* for mixtures as a function of composition *x* along the solvent's (pure water) critical isotherm-isochore and values of partial molar volumes $\bar{V}_2^\infty$ at infinite dilution have been calculated using the crossover equation of state. The values of derived Krichevskii parameter and partial molar volumes were compared with data reported in the literature. The value of the critical exponent ϵ for partial molar volumes $\bar{V}_2^\infty$ at infinite dilution along the water's critical isotherm-isobar ($\bar{V}_2^\infty \propto x^{-\epsilon}$, $\epsilon = 0.795 \pm 0.001$) was estimated from our experimental data. Using the present *PVTx* data together with data obtained earlier by other authors, we developed a crossover Helmholtz free-energy model (CREOS) for dilute aqueous *n*-hexane solutions in wide temperature and pressure ranges around the vapor−liquid critical points. The CREOS represents all available experimental *PVTx* data for a dilute $H_2O + n\text{-}C_6H_{14}$ mixture with an average absolute deviation (AAD) of about 0.50−0.65% in the temperature and density ranges $0.98T_c(x) \leq T \leq 1.15T_c(x)$ and $0.35\rho_c(x) \leq \rho \leq 1.65\rho_c(x)$, respectively, and concentrations up to 0.05 mole fractions of *n*-hexane.

Acknowledgment

The research in the Institute for Geothermal Problems of the Dagestan Scientific Center of RAS was supported by the Russian Fond of Basic Researches under Grant No. RFBR 03-02-16220. The research in the Colorado School of Mines was supported by the U.S. Department of Energy, Office of Basic Energy Sciences, under Grant No. DE-FG03-95ER14568.

Literature Cited

(1) Connolly, J. F. Solubility of Hydrocarbons in Water Near the Critical Solution Temperatures. *J. Chem. Eng. Data* **1966**, *11*, 13.

(2) Gao, J. Supercritical Hydration of Organic Compounds. The Potential of Mean Force for Benzene Dimer in Supercritical Water. *J. Am. Chem. Soc.* **1993**, *115*, 6893.

(3) Penniger, J. M. L. Extraction of Oil from Wyoming Coal with Aqueous Solvents at Elevated Pressures. In *Supercritical Fluid Technology*; Penniger, J. M. L., Rodosz, M., McHugh, M. A., Krukonis, V. J., Eds.; Elsevier: New York, 1987; pp 309−329.

(4) Naragan, R.; Antol, M. J. Kinetic Elucidation of the Acid-catalyzed Mechanism of Propanop-1 Dehydration in Supercritical Water. In *Supercritical Fluid Science and Technology*; Joohnston, K. P., Penninger, J. M. L., Eds.; American Chemical Society: Washington, DC, 1989; pp 226−241.

(5) G*uidelines for Phase Separations in High-Temperature and Supercritical Water Solutions*, A Report on a Workshop Organized by the US Army Research Office and the Forschungszentrum Karlsruhe; Shaw, R. W., Boukis, N., Eds.; 7−9 July 1999, Army Research Laboratory, Research Triangle Park, NC, 2000.

(6) Thomason, T. B.; Modell, M. Supercritical Water Destruction of Aqueous Wastes. *Hazard. Wastes* **1984**, *1*, 453.

(7) Staszak, C. N.; Malinaaski, K. C.; Killilea, W. R. The Pilot-Scale Demonstration of the MODAR Oxidation Process for the Destruction of Hazardous Organic Waste Materials. *Environ. Prog.* **1987**, *6*, 39.

(8) Shaw, R. V.; Brill, N. B.; Clifford, A. A.; Eckert, C. A.; Franck, E. U. Supercritical Water: A Medium for Chemistry. *Chem. Eng. News* **1991**, *69*, 36.

(9) Modell, M.; Gaudet, G. G.; Simson, M.; Hong, G. T.; Bieman, K. Supercritical Water. *Solid Wastes Manage.* **1982**, *26*, 30.

(10) Franck, E. U. Supercritical Water. In *Steam, Water, and Hydrothermal Systems*: Proc. of the 13th Int. Conf. Prop. of Water and Steam; Tremaine, P. R., Hill, Ph. G., Irish, D. E., Balakrishnan, P. V., Eds.; NRC Research Press: Ottawa, 2000; pp 22−34.

(11) Pitzer, K. S. Thermodynamic of Natural and Industrial Waters. *J. Chem. Thermodyn.* **1993**, *25*, 7.

(12) Cocero, M. J.; Vallelado, D.; Torio, R.; Alonso, E.; Fdez-Polanco, F. Optimization of the Operation Variables of a Supercritical Water Oxidation Process. *Water Sci. Technol.* **2000**, *42*, 107.

(13) Barner, H. E.; Huang, C. Y.; Johnson, T.; Jacobs, G.; Martch, M. A. Supercritical Water Oxidation: An Emerging Technology. *J. Hazard. Mater.* **1992**, *32*, 1.

(14) Tester, J. W.; Holgate, H. R.; Armellini, F. J.; Webley, P.; Killilea, W. R.; Hong, G. T.; Barner, H. E. Supercritical Water Oxidation Technology: A Review of Process Development and Fundamental Research. In *Emerging Technologies in Hazardous Waste Managment III*; Tedder, D. W., Pohland, F. G., Eds.; American Chemical Society: Washington, DC, 1993.

(15) Zakharov, A. S.; Kachalov, V. V.; Kiselev, S. B.; Chernomyrdin, A. V.; Shpilrain, E. E. Physical Simulation of the Processes of Displacement of Hydrocarbon Systems from a Porous Medium by Water under Critical Conditions. *High Temp.* **1997**, *35*, 96.

(16) Hawthorne, S. B. Analytical-Scale Supercritical Fluid Extraction. *Anal. Chem. A* **1990**, *62*, 633.

(17) Hawthorne, S. B.; Yang, Yu.; Miller, D. J. Extraction of Organic Pollutants from Environmental Solids with Sub- and Supercritical Water. *Anal. Chem.* **1994**, *66*, 2912.

(18) Chester, T. L.; Pinkston, J. D.; Raynie, D. E. Supercritical Fluids and Unified Chromatography. *Anal. Chem. R* **1992**, *64*, 153.

(19) Alexandrou, N.; Lawrence, M. J.; Pawliszyn, J. Cleanup of Complex Organic Mixtures Using Supercritical Fluids and Selective Absorbents. *Anal. Chem.* **1992**, *64*, 301.

(20) Siskin, M.; Katritzky, A. R. Reactivity of Organic-Compounds in Hot Water-Geochimical and Technological Implications. *Science* **1991**, *254*, 231.

(21) Levelt Sengers, J. M. H.; Morrison, G.; Nielson, G.; Chang, R. F.; Everhart, C. M. Thermodynamic Behavior of Supercritical Fluid Mixtures. *Int. J. Thermophys.* **1986**, *7*, 231.

(22) Chang, R. F.; Morrison, G.; Levelt Sengers, J. M. H. The Critical Dilemma of Dilute Mixtures. *J. Phys. Chem.* **1984**, *88*, 3389.

(23) Levelt Sengers, J. M. H. Solubility Near the Solvent's Critical Point. *J. Supercritical Fluids* **1991**, *4*, 215.

(24) Harvey, A. H.; Levelt Sengers, J. M. H. Unified Description of Infinite-Dilution Thermodynamic Properties for Aqueous Solutions. *J. Phys. Chem.* **1991**, *95*, 932.

(25) Levelt Sengers, J. M. H. Thermodynamics of Solutions Near the Solvent's Critical Point. In *Supercritical Fluid Technology*; Ely, J. F., Bruno, T. J., Eds.; CRC Press: Boca Raton, FL, 1991; p 1.

(26) Chang, R. F.; Levelt Sengers, J. M. H. Behavior of Dilute Mixtures Near the Solvent's Critical Point. *J. Phys. Chem.* **1986**, *90*, 5921.

(27) Chialvo, A. A.; Cummings, P. T. Solute-Induced Effects on the Supercritical Fluids and Thermodynamics of Infinitely Dilute Mixtures. *AIChE J.* **1994**, *40*, 1558.

(28) Cummings, P. T.; Chialvo, A. A. Molecular Simulation Study of Solvation Structure in Supercritical Aqueous Solutions. *Chem. Eng. Sci.* **1994**, *49*, 2735.

(29) Chialvo, A. A.; Cummings, P. T. Comment on "Near-Critical Phase Behavior of Dilute Mixtures". *Mol. Phys.* **1995**, *84*, 41.

(30) Debenedetti, P. G.; Kumar, S. K. The Molecular Basis of Temperature Effects in Supercritical Extractions. *AIChE J.* **1984**, *34*, 645.

(31) Debenedetti, P. G.; Mohamed, R. S. Attractive, Weakly Attractive, and Repulsive Near-Critical Systems. *J. Chem. Phys.* **1989**, *90*, 4528.

(32) McGuigan, D. B.; Monson, P. A. Analysis of Infinite Dilution Partial Molar Volumes Using a Distribution Function Theory. *Fluid Phase Equilib.* **1990**, *57*, 227.

(33) Chialvo, A. A.; Cummings, P. T. *Supercritical Water and Aqueous Solutions: Molecular Simulation. Encyclopedia of Computational Chemistry*; Wiley: New York, 1998; pp 2839−2859.

(34) Abdulagatov, I. M.; Bazaev, A. R.; Ramazanova, A. E. *PVTx* Properties and Virial Coefficients of the Water + n-Hexane System. *Ber. Bunsen-Ges. Phys. Chem.* **1994**, *98*, 1596.

(35) Abdulagatov, I. M.; Bazaev, E. A.; Bazaev, A. R.; Rabezkii, M. G. *PVTx* Measurements for Dilute Water + n-Hexane Mixtures in the Near-Critical and Supercritical Regions. *J. Supercrit. Fluids* **2001**, *19*, 219.

(36) Degrange, S. Nouvelle Procedure de Determination Simultanee des Proprietes Enthalpiques et Volumiques des Systemes Fluides: Application a L'etude des Solutions Aqueuses D'hydrocarbures Jusqu'au Domaine Critique de L'eau. Ph.D. Thesis, University Blaise Pascal, France, 1998.

(37) Yiling, T.; Michelberger, Th. M.; Franck, E. U. High-Pressure Phase Equilibria and Critical Curves of (Water + n-Butane) and (Water + n-Hexane) at Temperatures to 700 K and Pressures to 300 MPa. *J. Chem. Thermodyn.* **1991**, *23*, 105.

(38) Kamilov, I. K.; Malysheva, L. V.; Rasulov, A. R.; Shakhbanov, K. A.; Stepanov, G. V. Experimental Investigation of $C_{v,x}$,*P,V,T* Properties and the Equation of State of the n-Hexane + Water System. *Fluid Phase Equilib.* **1996**, *125*, 177.

(39) Kamilov, I. K.; Stepanov, G. V.; Abdulagatov, I. M.; Rasulov, A. R.; Milikhina, E. I. Liquid−Liquid−Vapor, Liquid−Liquid, and Liquid−Vapor Phase Transitions in Aqueous *n*-Hexane Mixtures from Isochoric Heat Capacity Measurements. *J. Chem. Eng. Data* **2001**, *46*, 1556.

(40) Kamilov, I. K.; Stepanov, G. V.; Malysheva, L. V.; Rasulov, A. R.; Rasulov, S. M.; Shakhbanov, K. A. Phase Equilibrium Curves and Critical Lines of n-Hexane + Water: Liquid−Liquid and Liquid−Gas. *High Temp.−High Press.* **1997**, *29*, 237.

(41) von Konynenburg, P. H.; Scott, P. L. Critical Lines and Phase Equilibria in Binary van der Waals Mixtures. *Philos. Trans. R. Soc. London A* **1980**, *298*, 495.

(42) Stepanov, G. V.; Shakhbanov, K. A.; Malysheva, L. V. Thermodynamic Properties of Water + n-Hexane Mixture at Critical and Supercritical Parameters. *High Temp.* **1997**, *35*, 192.

(43) De Loos, Th. W.; Penders, W. G.; Lichtenthaler, R. N. Phase Equilibria and Critical Phenomena in Fluid (n-Hexane + Water) at High Pressures and Temperatures. *J. Chem. Thermodyn.* **1982**, *14*, 83.

(44) De Loos, Th. W.; van Dorp, J. H.; Lichtenthaler, R. N. Phase Equilibria and Critical Phenomena in Fluid (n-Alkane + Water) Systems at High Pressures and Temperatures. *Fluid Phase Equilib.* **1983**, *10*, 279.

(45) Tsonopoulos, C.; Wilson, G. M. High-Temperature Mutual Solubilities of Hydrocarbons and Water. *AIChE J.* **1983**, *29*, 990.

(46) Brunner, E., IX. Phase Separation and Critical Phenomena in 23 (n-Alkane + Water) Mixtures. *J. Chem. Thermodyn.* **1990**, *22*, 335.

(47) Roof, J. G. Three-Phase Critical Point in Hydrocarbon + Water Systems. *J. Chem. Eng. Data* **1970**, *15*, 301.

(48) Rebert, C. J.; Hayworth, K. E. The Gas and Liquid Solubility Relations in Hydrocarbon + Water Systems. *AIChE J.* **1967**, *13*, 118.

(49) Scheffer F. E. C. On Unmixing in a Binary System for which the Three-Phase Pressure is Greater than the Sum of the Vapor Tensions of the Two Components. *Konikl. Akad. Wetenschap. Amsterdam* **1914**, *17*, 835.

(50) Victorov, A. I.; Fredenslund, Aa.; Smirnova, N. A. Fluid Phase Equilibria in Water: Natural Gas Component Mixtures and Their Description by the Hole Group-Contribution Equation of State. *Fluid Phase Equilib.* **1991**, *66*, 187.

(51) Neichel, M.; Franck, E. U. Critical Curve and Phase Equilibria of Water + n-Alkane Binary Systems to High Pressures and Temperatures. *J. Supercrit. Fluids* **1996**, *9*, 69.

(52) Heilig, M.; Franck, E. U. Calculation of Thermodynamic Properties of Binary Fluid Mixtures to High Temperatures and High Pressures. *Ber. Bunsen-Ges. Phys. Chem.* **1989**, *93*, 898.

(53) Heilig, M.; Franck, E. U. Phase Equilibria of Multicomponent Fluid Systems to High Pressures and Temperatures. *Ber. Bunsen-Ges. Phys. Chem.* **1990**, *94*, 27.

(54) Wormald, C. J.; Colling, C. N.; Lancaster, N. M.; Sellars, A. J. *Excess Enthalpy Experimental Data. Binary Systems: Water + n-Pentane, Water + n-Hexane, Water + n-Heptane, and Water + n-Octane*; Research Report RR-68; Gas Processors Association: Tulsa, OK, 1983.

(55) Wormald, C. J.; Lancaster, N. M. Excess Enthalpies and Cross-Term Second Virial Coefficients for Mixtures Containing Water Vapor. *J. Chem. Soc., Faraday Trans. I* **1988**, *84*, 3141.

(56) Wormald, C. J. Heats of Mixing of Water + Hydrocarbons at High Temperatures and Pressures. *Ber. Bunsen-Ges. Phys. Chem.* **1984**, *88*, 826.

(57) Majer, V.; Degrange, S.; Sedlbauer, J. Temperature Correlation of Partial Molar Volumes of Aqueous Hydrocarbons at Infinite Dilution: Test of Equations. *Fluid Phase Equilib.* **1999**, *158−160*, 419.

(58) Abdulagatov, I. M.; Bazaev, A. R.; Gasanov, R. K.; Ramazanova, A. E. Measurements of the *PVT* Properties and Virial Coefficients of Pure Water, Methane, n-Hexane, n-Octane, Benzene, and Their Aqueous Mixtures in the Critical Region. *J. Chem. Thermodyn.* **1996**, *28*, 1037.

(59) Abdulagatov, I. M.; Bazaev, A. R.; Gasanov, R. K.; Bazaev, E. A.; Ramazanova, A. E. Measurements of the *PVTx* Properties of n-Heptane in Supercritical Water. *J. Supercrit. Fluids* **1997**, *10*, 149.

(60) Abdulagatov, I. M.; Bazaev, A. R.; Gasanov, R. K.; Bazaev, E. A.; Ramazanova, A. E. Pressure, Volume, Temperature, and Composition Measurements and Thermodynamic Properties of Water + n-Heptane Mixtures in the Supercritical Regions. *High Temp.-High Press.* **1997**, *29*, 137.

(61) Abdulagatov, I. M.; Bazaev, A. R.; Bazaev, E. A.; Khokhlachev, S. P.; Saidakhmedova, M. B.; Ramazanova, A. E. Excess, Partial, and Apparent Molar Volumes of n-Alkanes in Near- and Supercritical Water. *J. Solution Chem.* **1998**, *27*, 729.

(62) Abdulagatov, I. M.; Bazaev, A. R.; Bazaev, E. A.; Saidakhmedova, M. B.; Ramazanova, A. E. Volumetric Properties of Near- and Supercritical Water + *n*-Pentane Mixtures: Excess, Partial, and Apparent Molar Volumes. *J. Chem. Eng. Data* **1998**, *43*, 451.

(63) Abdulagatov, I. M.; Bazaev, A. R.; Bazaev, E. A.; Saidakhmedova, M. B.; Ramazanova, A. E. *PVTx* Measurements and Partial Molar Volumes for Water + Hydrocarbon Mixtures in the

Near-Critical and Supercritical Conditions. *Fluid Phase Equilib*. **1998**, *150*, 537.

(64) Bazaev, A. R.; Abdulagatov, I. M.; Magee, J. W.; Rabezkii, M. G.; Bazaev, E. A. Rabezkii, M. G. *PVT* Measurements for Toluene in the Near-Critical and Supercritical Regions. *J. Chem. Eng. Data* **2001**, *46*, 1089.

(65) Rabezkii, M. G.; Bazaev, A. R.; Abdulagatov, I. M.; Magee, J. W.; Bazaev, E. A. *PVTx* Measurements for Water + Toluene Mixtures in the Near-Critical and Supercritical Regions. *J. Chem. Eng. Data* **2001**, *46*, 1610.

(66) Bazaev, A. R.; Abdulagatov, I. M.; Magee, J. W.; Bazaev, E. A.; Ramazanova, A. E. *PVTx* Measurements for H_2O+D_2O Mixtures in the Near-Critical and Supercritical Regions. *J. Supercrit. Fluids* **2003**, *26*, 115.

(67) Wagner, W.; Pruss, A. The IAPWS Formulation 1995 for the Thermodynamic Properties of Ordinary Water Substance for General and Scientific Use. *J. Phys. Chem. Ref. Data* **2002**, *31*, 387.

(68) Tsiklis, D. S.; Linshiz, L. R.; Rodkina, I. B. Measurements of the Molar Volumes of Gaseous Mixtures at High Pressures. *Thermophys. Prop. Subst. Mater.* **1969**, *2*, 268.

(69) Keyes, F. G.; Smith, L. B. An Experimental Thermodynamic Investigation of Electrolyte Solutions. *Proc. Am. Acad. Arts Sci.* **1933**, *68*, 505.

(70) Bazaev, A. R. The System of Automatic Regulating of Temperature in Air Space. *Heat Transfer* **1988**, *1*, 113.

(71) Higashi, H.; Furuya, T.; Ishidao, T.; Iwai, Y.; Arai, Y. An Exponent Type Mixing Rule for Energy Parameters. *J. Chem. Eng. Jpn.* **1994**, *27*, 677.

(72) Haruki, M.; Iwai, Y.; Nagao, S.; Yahiro, Y.; Arai, Y. Measurement and Correlation of Phase Equilibria for Water + Hydrocarbon Systems near the Critical Temperature and Pressure of Water. *Ind. Eng. Chem. Res.* **2000**, *39*, 4516.

(73) Haruki, M.; Yahiro, Y.; Nigashi, H.; Iwai, Y.; Arai, Y. Correlation of Phase Equilibria for Water + Hydrocarbon Systems at High Temperatures and Pressures by Cubic Equation of State. *J. Chem. Eng. Jpn.* **1999**, *32*, 535.

(74) Kiselev, S. B. Prediction of the Thermodynamic Properties and the Phase Behavior of Binary Mixtures in the Extended Critical Region. *Fluid Phase Equilib.* **1997**, *128*, 1.

(75) Kiselev, S. B.; Rainwater, J. C. Extended Law of Corresponding States and Thermodynamic Properties of Binary Mixtures in and Beyond the Critical Region. *Fluid Phase Equilib.* **1997**, *141*, 129.

(76) Kiselev, S. B.; Rainwater, J. C. Enthalpies, Excess Volumes, and Specific Heats of Critical and Supercritical Binary Mixtures. *J. Chem. Phys.* **1998**, *109*, 643.

(77) Kiselev, S. B.; Ely, J. F.; Abdulagatov, I. M.; Bazaev, A. R.; Magee, J. W. Equation of State and Thermodynamic Properties of Pure Toluene and Dilute Aqueous Toluene Solutions in the Critical and Supercritical Regions. *Ind. Eng. Chem. Res.* **2002**, *41*, 1000.

(78) Griffiths, R. B.; Wheeler, J. C. Critical Points in Multicomponent System. *Phys. Rev. A* **1970**, *2*, 1047.

(79) Kiselev, S. B.; Kostyukova, I. G.; Povodyrev, A. A. Universal Crossover Behavior of Fluids and Fluid Mixtures in the Critical Region. *Int. J. Thermophys.* **1991**, *12*, 877.

(80) Kiselev, S. B. Universal Crossover Functions for the Free Energies of Single-Component and Two-Component Fluids in Their Critical Regions. *High Temp.* **1990**, *28*, 47.

(81) Kiselev, S. B.; Sengers, J. V. An Improved Parametric Crossover Model for the Thermodynamic Properties of Fluids in the Critical Region. *Int. J. Thermophys.* **1993**, *14*, 1.

(82) Landau, L. D.; Lifshitz, E. M. *Statistical Physics, Part 1*; Pergamon Press: New York, 1980.

(83) Patashinskii, A. Z.; Pokrovskii, V. L. *Fluctuation Theory of Phase Transitions*, 3rd ed.; Pergamon: New York, 1979.

(84) Anisimov, M. A.; Kiselev, S. B.; Sengers, J. V.; Tang S. Crossover Approach to Global Critical Phenomena in Fluids. *Physica A* **1992**, *188*, 487.

(85) Kiselev, S. B.; Rainwater, J. C.; Huber, M. L. Binary Mixtures in and Beyond the Critical Region: Thermodynamic Properties. *Fluid Phase Equilib.* **1998**, *150*−*151*, 469.

(86) Kiselev, S. B.; Huber, M. L. Thermodynamic Properties of R32 + R134a and R125 + R32 Mixtures in and Beyond the Critical Region. *Int. J. Refrig.* **1998**, *21*, 64.

(87) Kiselev, S. B.; Abdulagatov, I. M.; Harvey, A. H. Equation of State and Thermodynamic Properties of Pure D2O and D2O + H2O Mixtures In and Beyond the Critical Region. *Int. J. Thermophys.* **1999**, *20*, 563.

(88) Kiselev, S. B.; Povodyrev, A. A. An Isomorphic Generalization of the Law of Corresponding States for Binary Mixtures. *Fluid Phase Equilib.* **1992**, *79*, 33.

(89) Kiselev, S. B.; Friend, D. G. Revision of a Multiparameter Equation of State to Improve the Representation in the Critical Region: Application to Water. *Fluid Phase Equilib.* **1999**, *155*, 3.

(90) Kurumov, D. S.; Grigor'ev, B. A. Experimental Study of *PVT*-Dependence of *n*-Hexane in the Critical Region. *Russ. J. Phys. Chem.* **1982**, *56*, 551.

(91) Kurumov, D. S.; Grigor'ev, B. A. Experimental Study of the Thermal Properties of n-Hexane at High Temperatures and Pressures. *Izv. Vys. Ucheb. Zaved. Neft i Gas* (in Russian) **1983**, *26*, 35.

(92) Amirkhanov, Kh. I.; Alibekov, B. G.; Vikhrov, D. I.; Mirskaya, V. A. *Isochoric Heat Capacity and Other Caloric Properties of Hydrocarbons*; DSC RAS: Makhachkala, 1981.

(93) Span, R., *Multiparameter Equations of State-an Accurate Source of Thermodynamic Property Data*; Springer: Berlin, 2000.

(94) Polt, A.; Platzer, B.; Maurer, G. Parameter der Thermischen Zustandsgleichung von Bender für 14 Mehratomige Reine Stoffe. *Chem. Tech.* (*Leipzig*) **1992**, *44*, 216.

(95) Starling, K. E. *Fluid Thermodynamic Properties for Light Petroleum Systems*; Gulf Publ. Co.: Houston, TX, 1973.

(96) Grigor'ev, B. A.; Rastorguev, Yu. L.; Kurumov, D. S.; Gerasimov, A. A.; Kharin, V. E.; Plotnikov, D. S. Thermodynamic Properties of n-Hexane. *Int. J. Thermophys.* **1988**, *9*, 439.

(97) Grigor'ev, B. A.; Rastorguev, Yu. L.; Gerasimov, A. A.; Kurumov, D. S.; Plotnikov, S. A. *n-Hexane. Thermodynamic Properties at Temperatures from 180 to 630 K and at Pressures Between 0.1 and 100 MPa*; GSSSD: Moscow, 1986.

(98) Gerasimov, A. A. Study of C_P of n-Hexane in the Region of Maximum of Heat Capacity. *Izv. Vys. Ucheb. Zaved. Neft i Gas* (in Russian) **1980**, *1*, 61.

(99) Wormald, C. J.; Yerlett, T. K. A New Enthalpy-Increment Calorimeter. Enthalpy Increments for n-Hexane. *J. Chem. Thermodyn.* **1985**, *17*, 1171.

(100) Plyasunov, A. V.; Shock, E. L. Estimation of the Krichevskii Parameter for Aqueous Nonelectrolytes. *J. Supercrit. Fluids* **2001**, *20*, 91.

(101) Plyasunov, A. V.; Shock, E. L. Prediction of the Vapor-Liquid Distribution Constants for Volatile Nonelectrolytes in Water up to its Critical Temperature. *Geochim. Cosmochim. Acta* **2004**, *67*, 4981.

(102) Abdulagatov, I. M.; Dadashev, M. N.; Saidalhmedova, M. B. Study of the Thermodynamic Behavior of Dilute Solutions Near the Solvent's Critical Point on the Basis of Critical Line Data. *Russ. Chem. Chem. Prod.* **1998**, *1*−*2*, 30.

(103) Fisher, M. E. Renormalization of Critical Exponents by Hidden Variables. *Phys. Rev.* **1968**, *176*, 237.

(104) Saam, W. F. Thermodynamics of Binary Systems Near the Liquid−Gas Critical Point. *Phys. Rev. A* **1970**, *2*, 1461.

(105) Anisimov, M. A.; Voronel, A. V.; Gorodetskii, E. E. Isomorphism of Critical Phenomena. *Sov. Phys. JETP* **1971**, *33*, 605.

(106) Anisimov, M. A.; Kiselev, S. B. Universal Crossover Approach to Description of Thermodynamic Properties of Fluids and Fluid Mixtures. In *Sov. Tech. Rev. B. Therm. Phys., Part 2*; Scheindlin, A. E., Fortov, V. E., Eds.; Harwood Academic: New York, 1992; pp 1−121.

(107) Kiselev, S. B. Scaled Equation of State of Single-Component Liquids and Binary Solutions in the Critical Region. *High Temp.* **1988**, *26*, 337.

(108) Kiselev, S. B.; Friend, D. G. Cubic Crossover Equation of State for Mixtures. *Fluid Phase Equilib.* **1999**, *162*, 51.

(109) Wormald, C. J.; Colling, C. N. Excess Enthalpies of Some Binary Steam Mixtures. In *Thermodynamics of Aqueous Systems with Industrial Applications*; ACS Symposium Series 133; American Chemical Society: Washington, DC, 1980; pp 435−447.

(110) Smith, G. R.; Fahy, M. J.; Wormald, C. J. The Excess Molar Enthalpy of $\{xH_2O+(1-x)C_nH_{2n+2}\}$ (g) for n=5, 6, 7, and 8. *J. Chem. Thermodyn.* **1984**, *16*, 825.

(111) Eubank, P. T.; Wu, C. H.; Alvarado, J. F. J.; Forero, A.; Beladi, M. K. Measurements and Prediction of Three-Phase Water/Hydrocarbon Equilibria. *Fluid Phase Equilib.* **1994**, *102*, 181.

(112) Kurumov, D. S. Thermal Properties of n-Alkanes and Oil Fractions in Liquid and Gaseous Phases. Ph.D. Thesis, MEI: Moscow, 1991.

(113) Genco, J. M.; Teja, A. S.; Kay, W. B. Study of the Critical and Azeotropic Behavior of Binary Mixtures. 2. *PVT-x* Data and Azeotropic States of Perfluoromethylcyclohexane-Isomeric Hexane Systems. *J. Chem. Eng. Data* **1980**, *25*, 355.

(114) Rathmann, D.; Sullivan, D. A.; Thompson, P. A. *Liquid−Vapor Saturation Data*; Max-Planck Institut für Strömungsforschung: Göttingen, 1979.

(115) Cibulka, I. Saturated Liquid Densities of 1-Alkanols from C_1 to C_{10} and n-Alkanes from C_5 to C_{16}: A Critical Evaluation of Experimental Data. *Fluid Phase Equilib.* **1993**, *89*, 1.

(116) Thomas, G. L.; Young, S. The Vapor Pressures, Specific Volumes and Critical Constants of Normal Hexane. *J. Chem. Soc.* **1895**, *67*, 1071.

(117) Sauermann, P.; Holzapfel, K.; Oprzynski, J.; Kohler, F.; Poot, W.; de Loos, Th. W. The *PρT* Properties of Ethanol-Hexane. *Fluid Phase Equilib.* **1995**, *112*, 249.

(118) Mousa, A. H. N. The Physical Properties of Highly Purified Samples of Propane and n-Hexane. *J. Chem. Thermodyn.* **1977**, *9*, 1063.

(119) Shim, J.; Kohn, J. P. Multiphase and Volumetric Equilibria of Methane−*n*-Hexane Binary System at Temperatures Between −110° and 150 °C. *J. Chem. Eng. Data* **1962**, *7*, 3.

(120) Kay, W. B. The Vapor Pressures and Saturated Liquid and Vapor Densities of the Isomeric Hexanes. *J. Am. Chem. Soc.* **1946**, *68*, 1336.

(121) Grigor'ev, B. A.; Gerasimov, A. A.; Kurumov, D. S.; Vasil'ev, Yu. P. Study of the Thermodynamic Properties of *n*-Hexane Along the Coexistence Curve. *Ul'trazvuk i Fiziko-Khimicheskie Svoistva Veshestv*; Kursk Pedagogical Institute: Kursk, 1983; pp 22−29.

(122) de Loos, Th. W.; Poot, W.; de Swaan Arons, J. Vapor-Liquid Equilibria and Critical Phenomena in Methanol-n-Alkane Systems. *Fluid Phase Equilib.* **1988**, *42*, 209.

(123) Kay, W. B. Vapor-Liquid equilibrium Relationships of Binary Systems. *J. Chem. Eng. Data* **1971**, *16*, 137.

(124) Zotov, V. V.; Neruchev, Yu. A. *Ultrasonic and Thermodynamic Properties of Substances*; Kursk Pedagogical Institute: Kursk, 1986; pp 34−42.

(125) Mel'nikov, G. A.; Verveiko, V. N.; Otpushennikov, N. F. Comprehensive Study of Elastic and Caloric Properties of Hydrocarbons by Acoustic Method. *Russ. J. Phys. Chem.* **1988**, *62*, 798.

(126) Mustafaev, P. A. *Thermophysical Properties of Hydrocarbons at High Parameters of State*; Energoatomizdat: Moscow, 1981.

(127) Amirkhanov, Kh. I.; Alibekov, B. G.; Vikhrov, D. I.; Mirskaya, V. A.; Levina, L. N. Isobaric Heat Capacity of n-Pentane, n-Hexane, n-Heptane, and n-Octane Along the Coexistence Curve. *High Temp.* **1971**, *6*, 1310.

(128) Gerasimov, A. A.; Grigor'ev, B. A.; Rastorguev, Yu. L. Isobaric Heat Capacity of n-Hexane at Pressures Below Critical Value. *Izv. Severo-Kavkas. Nauch. Zentra Vyshei Shkoly, ser. Tekh. Nauk.* **1979**, *4*, 72.

(129) Abdulagatov, I. M.; Dvoryanchikov, V. I.; Kamalov, A. N. Heat Capacities at Constant Volume of Pure Water in the Temperature Range 412−693 K at Densities from 250 to 925 $kg \cdot m^{-3}$. *J. Chem. Eng. Data* **1998**, *43*, 830.

(130) Abdulagatov, I. M.; Mursalov, B. A.; Gamzatov, N. M. Isochoric Heat Capacity of Water in the Vicinity of the Critical Point Including the Metastable Region. In *Physical Chemistry of Aqueous Systems. Proc. 12th Int. Conf. Prop. Water and Steam*; White, H., Sengers, J. V., Neumann, D. B., Bellows, J. C., Eds.; Begell House: New York, 1995; pp 94−102.

Received for review July 26, 2004
Revised manuscript received November 23, 2004
Accepted December 6, 2004

IE049339A